RAPID PROTOTYPING, RAPID TOOLING AND DIGITAL PHOTOELASTICITY : AN INTEGRATED APPROACH

by

M. Anil Kumar

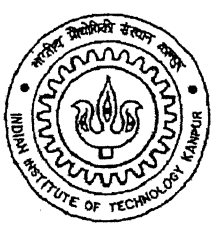

DEPARTMENT OF MECHANICAL ENGINEERING
INDIAN INSTITUTE OF TECHNOLOGY KANPUR
AUGUST 1998

RAPID PROTOTYPING, RAPID TOOLING AND DIGITAL PHOTOELASTICITY : AN INTEGRATED APPROACH

A Thesis Submitted in
Partial Fulfillment of the Requirements
for the degree of

MASTER OF TECHNOLOGY

by

M. Anil Kumar

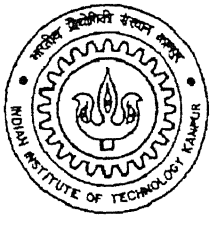

DEPARTMENT OF MECHANICAL ENGINEERING
INDIAN INSTITUTE OF TECHNOLOGY KANPUR
AUGUST 1998

DEDICATED TO MY PARENTS

CERTIFICATE

This is to certify that the work contained in the thesis entitled, "**RAPID PROTOTYPING, RAPID TOOLING AND DIGITAL PHOTOELASTICITY : AN INTEGRATED APPROACH**", by *M. ANIL KUMAR* has been carried out under our supervision and that this work has not been submitted elsewhere for a degree.

Dr. S. G. Dhande
Professor,
Dept. of Mechanical Engg.,
I.I.T. Kanpur.

Dr. K. Ramesh
Associate Professor,
Dept. of Mechanical Engg.,
I.I.T. Kanpur.

August, 1998

TABLE OF CONTENTS

ACKNOWLEDGEMENTS

I am indebted to Dr. Sanjay G. Dhande and Dr. k. Ramesh for their excellent guidance and fruitful discussions during the current work. I am thankful to them for assisting me in the successful and in time completion of the work. I am specially thankful to Dr. Dhande for giving me the opportunity to work with the leading end technologies like RP & RT. Working close to the industry and in an open work environment under the able leadership of Dr. Dhande was a very fruitful learning experience. I would like to thank Dr. K. Ramesh who was always approachable for comments and discussions during any time of the day.

I would to like place on record my thanks to Dr. R. K. Singh, Deputy Director, DMSRDE, Kanpur for the informative discussions I had with him.

I am thankful to Shri A. D. Bhatt for the his help rendered in the form of suggestions and technical discussions. I am also thankful to Shri C.P.Singh, Technical officer CAD-P, Lab for providing the necessary things in the lab. Thanks are also due to Shri Surendra Gupta, Shri Babulal and Shri Sarju for their help rendered to me at the CAD Lab.

I express my gratitude to Shri S. K. Mangal who has always extended a helping hand in times of need. Thanks are due to Shri Radhesham without whose assistance it would have been difficult to carry out the experiments.

It was an enjoyable life at the CAD Lab with Sridharan(Muralidhar), Rahul(Manti), Rajkumar(Birru) and Manojji , not to forget the sleepless nights spent either completing the projects, playing with the computers or surfing the WWW. My special thanks are due to Sridharan and Rahul who have helped me testing times. Dantam and Nadham were of immense help in the Photoelasticity lab aiding me to complete the work. I am indebted to the whole CAD lab TEAM for their excellent co-operation and help extended during my stay at the lab.

Special thanks are to our administrator saab Siddharth Dubey who has provided me with the facilities at the times of need. I am specially thankful to Rahul, Manoj, Lsri, Karvind and chandu (lambu) for their help during my thesis write-up.

A - 210 in Hall 4 will always be a memorable one with fond memories of Bal, Avesham, Chotu, Shiva and Jeevan Madhu. I am specially thankful to this team who have helped me out when I had a fractured ankle. Thanks are due to my predecessors Jagan, Kanth, Gorti, Satish, Sridhar and Eswar for their helpful suggestions. I am also thankful to Rameshwar, Raju, Murthy, Shiva Rama Krishna, Badugu, Yarram and chalam, for making life enjoyable and a memorable one at IIT-K. I would like to thank the Badminton team of Srinivas, Satyam, Niranjan for taking the pains of waking me up daily in the morning.

I would also like to thank one and all who have assisted me in the one and a half year stay at IIT. May I be forgiven if I have missed out any of the names.

Anil

LIST OF FIGURES

LIST OF TABLES

ABSTRACT

The recent advances in data acquisition techniques based on digital image processing technology have made photoelastic stress analysis faster and the use of computer graphics for fringe reconstruction has made the analysis internally self-consistent. However, one of the main bottlenecks in 3D photoelastic analysis is the skill needed to prepare a 3D model. Further, for each loading condition, one needs an additional model for stress-freezing. Recent research on computer aided design and manufacturing has seen the development of a new technology called Rapid Prototyping. Among the various technologies available, Stereolithography(STL) found initial acceptance by photoelasticians because of its ability to provide models that are photoelastically sensitive. It is well known that the cost of a stereolithography system is quite high and cost-effective technologies were later developed for RP.

In the present work the Fused Deposition Modelling(FDM) and Solid Ground Curing(SGC) technologies are used for making photoelsatic models. In FDM the component is made by depositing a thermoplastic material such as ABS 400 layer by layer. In SGC acrylic based photopolymers are used to make the model by curing the liquid resin by Ultraviolet (UV) light. The models made directly by these processes are not directly suitable for analysis. However if Rapid Prototyping based on FDM or SGC is coupled with Rapid Tooling - one can make models that are photoelastically sensitive.

The first major step was the identification of the resin suitable for photoelastic analysis. It is demonstrated that SG 95 resin provided by HEK GmbH,(Germany) is an idle choice for the photoelastic stress analysis. The initial bottleneck to the process was the large amount of residual stress locked in the models from Rapid Tooling. A significant reduction in the residual stress has been achieved in the models made from the RT process by changing the ratio of mixing of the two components of the resin. Feasibility of the SG95 resin model for stress-freezing was also analyzed and the results were very encouraging.

Chapter 1

INTRODUCTION

1.1 TRADITIONAL METHODS OF MODEL MAKING

The most time-consuming and costly stage of a new product development is making a physical model or prototype of a design concept. Prototyping allows a designer to check the function and appearance of a part. The traditional methods generally used in industries are Casting, Forging and Machining. The procedure for traditional method of prototyping involves conceptual designing, drafting, model manufacturing and inspection. This requires pattern/die making, which are made-up of wood, wax, plaster of paris, etc. But, pattern/die making needs high human skill and experience, which is a main drawback of traditional methods. Complex parts having intricate internal shapes cannot be manufactured easily. So, there remains a geometrical inaccuracy in the prototype, which leads to inaccurate results. Apart from geometrical inaccuracies, traditional methods require special tools, jigs, fixtures and special purpose machines, which increases the cost of the end product and also the time taken to the market.

1.2 RAPID PROTOTYPING APPROACH OF MODEL MAKING

During the last decade, a class of technologies has emerged by which a computer-aided design file of an object can be converted into a physical model through special sintering, layering or deposition techniques, which are variously called as Rapid Prototyping (RP) [1], Solid free-form fabrication or Automated fabrication. The major application of this technology is the early verification of product designs and quick production of prototypes for testing. Changes made in early design and prototype phases have the greatest potential to improve or impair the end results. Multiple prototypes can now be reproduced more economically by using the RP as a master pattern for creating molded or soft tooling. RP allows designer to build tangible models of their designs quickly and cheaply. This encourages experimentation and flag errors in the fit or assembly of the part.

The **key benefits** that can be achieved through the use of RP technology are;

- The designer can prototype a part several times with slight variations, if necessary. This allows the design to be optimized and saves times-consuming and expensive alterations at a later stage.
- The ability to perform more up-front analysis eliminating errors while optimizing design for increased performance.
- RP technology reduces the need for traditional time-consuming tooling and cutting processes, need of jigs, fixtures and special purpose machines.
- By taking advantage of 3D CAD systems and RP technology, an industry can improve its design quality [2], shorten its production and manufacturing cycle times, improve its CAD database integrity and reduce its product costs.

Thus, RP bridges the gap between the design and manufacturing stages of a new product and helps to speed-up and automate the verification and tooling phase of the cycle.

1.3 RAPID TOOLING

Rapid tooling [3], a technology that adopts rapid prototyping techniques and applies them to tool and die making, is becoming an increasingly attractive alternative to traditional machining. Rapid tooling typically requires several steps to create the tool or die. In the indirect method of RT, a pattern is created by RP and used to form the tool. The other type of RT, the direct RT, produces the tool directly by the RP process.

When effectively implemented within a concurrent engineering environment, RT has the potential to dramatically improve the speed and cost of product development. Using computer-aided design, electronic data transfer, process simulation, and RT technologies, tooling costs and development times can be reduced by 75% or more. RT is especially useful when tool geometry makes traditional machining difficult because of part complexity or specific geometric features such as undercuts.

Room temperature vulcanisation (RTV) silicone rubber enables fabrication of flexible molds which can be used for manufacturing parts with intricate detail and

undercuts. Silicone rubber molds have excellent chemical resistance, low shrinkage and high dimensional stability, making them suitable for producing parts in polyester, epoxy and polyurethane.

The most widely used materials for producing rapid tooling components include thermosetting polymers: epoxy resins, polyurethanes (elastomers and foams) and silicones. Metals, especially those with the low melting alloys are also used in some processes. Some of the important operations employed for rapid tooling are epoxy resin casting, laminated shell molding, silicone rubber molding, polyurethane casting and metal arc spraying.

RT is not without its growing pains. The technology has limitations in accuracy, speed and capability that constrain its current applicability to prototype and low-volume tooling. These limitations are being addressed in development efforts and are expected to be mitigated in the near future. As the technology becomes more user friendly and robust, RT will not require such a high level of expertise.

1.4 RT MODELS FOR DESIGN ANALYSIS.

Component performance prediction by design analysis is a vital part of the development process and an area where SLA (Stereolithography) can play a vital role. The performance of many components is only verified by testing prototype parts, a stage that comes late in development phase, leaving little time for amendments to be made to the design. An alternative approach that has been developed at Indian Institute of Technology - Kanpur is to use RT models directly to perform empirical design analysis tests such as photoelastic analysis. Photoelastic techniques [4] can show high stress points in a component allowing design modification to be made very early on. Thus, the errors can be identified early in the design cycle, avoiding costly corrections in the post-prototyping stage.

1.5 PHOTOELASTIC ANALYSIS

Accurate analysis of prototypes is as important as its manufacturing. A design process is complete only if the prototypes are validated for its structural response under operating loads. Thus the stress analysis of rapid tooling models is crucial and

the technology chosen must be such the testing time is quite short. Among various experimental stress analysis tools, the whole field techniques are ideal to make measurements over large model area quickly.

The photoelastic analysis is a handy tool in this direction. Photoelasticity is an experimental method for analyzing stress/strain fields in mechanics. It has been successfully applied for analysis of prototypes. These models enable to conduct stress/strain analysis on real parts, operating under actual service conditions. Photoelasticity provides as no other existing method does, with an immediate practical solution of fundamental problems concerning stresses in element of structures and machines which cannot be directly observed and which are usually beyond the reach of calculation. Although the principles of photoelastic analysis have been known for more than a century and half, the practical applications would be workable only after more sensitive and easily workable materials are available. With the development of newer resins and their use as model material and further developments of technologies like RP & RT, photoelasticity found ever growing applications. A brief account of the new photoelastic materials and their feasibility to photoelastic response are discussed in this work. The discovery of "stress-freezing" technique for three-dimensional analysis opened an entirely new field, enabling solution of complex practical structural design problems.

1.6 STATEMENT OF PROBLEM

A careful selection of appropriate photoelastic resins is necessary for analysis of RT models. This thesis presents a systematic study on the Fusion of Rapid Tooling, Rapid Prototyping and Digital Photoelastic techniques, to better and faster stress analysis.

The main aim of this thesis is to set a well-defined methodology for photoelastic analysis of RT models, which is divided into four areas:

- **Rapid prototype pattern making**
- **Rapid Tooling model making**
- **Experimental analysis of RT models using Photoelasticity**
- **Comparison of experimental results with the Finite Element Analysis**

1.7 THESIS LAYOUT

Chapter 1 gives the general introduction about the topic. The procedure for creating computer-aided solid model of prototype using parametric solid modelling tool and pre-processing of this CAD model is discussed in Chapter 2. The Fused Deposition Modelling (FDM) technique and Solid Ground Curing (SGC) technique is also described in Chapter 2, which has been undertaken for experimental purpose.

In Chapter 3, the procedure to prepare the Rapid Tooling prototype for digital photoelastic analysis is described in detail.

The feasibility for stress analysis of the models made by the Rapid Tooling processes are discussed in Chapter 4. A circular disk was used to calibrate the material and a complex model namely a turbine blade was analysed for photoelastic response. There was a high amount of residual stress locked in the model in the preliminary analysis. Through further experimentation the residual stress levels were lowered the procedure for which is discussed in detail in Chapter 4.

Finally, the thesis ends with the conclusion and suggestions for future work in Chapter 5.

Chapter 2

MODEL MAKING USING RAPID PROTOTYPING

2.1 INTRODUCTION

From engineering designers to artists to chemists to biologists to doctors all of them strive to find tools to create new thoughts, new ideas and new inventions. For a marketing success or a faster analysis of critical components with new design it is crucial that this power of mind is utilized through better visualization tools. Computer graphics has evolved over the years to provide to better tools to create new things in abstract space. These objects are referred to as "VIRTUAL PROTOTYPES". Rapid prototyping is a layer by layer 'material increase' or 'material grow' or 'material incress manufacturing process. In these RP processes the final object is obtained by either gradual addition of material or by gradual binding or solidification or polymerization of material according to the requirements of the process.

Traditional mechanical engineering manufacturing techniques use subtractive methods in the fabrication process. In contrast, rapid prototyping is characterized by using additive methods. Small fabrication primitives, such as drops or layers, are applied over and over until the part is completed.

In this work use was made of FDM1650 (FUSED DEPOSITION MODELLING) machine of Stratasys Inc., and SOLIDER 4600 (Solid Ground Curing Technology) of Cubital Inc., available in the CAD-P laboratory IIT Kanpur. The details of these two processes are discussed herewith in detail.

2.2 FUSED DEPOSITION MODELLING (FDM)

Fused deposition modelling is an additive process that uses a layer as a manufacturing primitive to build a model. The model is built layer by layer using a thin wire of thermoplastic polymer namely ABS (Acrylonitrile Butadiene Styrene). The material filament is pulled into the FDM head by the drive wheels. It enters the

liquefier where it is heated until the material reaches a near-liquid state. As the material comes out of the nozzle tip, it bonds to previously deposited material. The deposited material is then allowed to cure in the closed cabinet at 70° C, which takes few seconds.

The basic input for any rapid prototyping process is an STL (stereolithography) file that is obtained from a CAD model. The geometric modelling of the objects in computer aided design can be done using three methods viz., wireframe modelling, solid modelling and surface modelling. The wireframe modeling approach is not appropriate for STL creation, as it does not have the volumetric data. Solid modelling is very useful in the creation of volumetric object and hence helpful for STL creation. The solid modelling packages which are used in the present work include Pro-Engineer and IDEAS. Pro-Engineer is based on the parametric technology, which requires all the dimensions to be specified before hand. Whereas IDEAS is based on variational technology which means that one can do any operations on the model without specifying the dimensions in the initial stages. This variational technology could prove helpful in conceptual design wherein one can proceed with the ideas in his mind without any dimensions. At any stage the model can be edited for adding the dimensions and all the operations done on the model will be updated immediately.

2.2.1 STL FILE FORMAT

All the rapid prototyping systems take the STL (Stereolithography) file as input. The STL file format lists the triangles of the outer shell of the solid model. Each triangle in the STL file format lists the normal vector of the triangle and x, y, z co-ordinates of the three vertices in free format. One of the many drawbacks of the STL file standard is that files tend to be quite voluminous. A new standard called a SOLI file has been developed by Cubital Inc., which reduces the amount of memory occupied, by a file.

The model accuracy depends on the triangulation of the STL file. Insufficient triangulation happens when not enough triangles are used to approximate the curved surfaces and surface types that have curvature in two directions like spheres, bicubic

surface patches and the turbine blade, a component that is being considered for the present analysis.

With the increase in the number of triangles the error decreases. The number of triangles to be taken is the discretion of the user and is controlled by parameters in the solid modelling packages. The biggest difficulty in generating the STL files is in the **Vertex-to-Vertex rule,** which states that:

Each edge in an STL file must be there between two and only two triangles.

2.2.2 FDM Hardware

The FDM1650 is a bench-top unit and can be placed next to a CAD workstation (Fig.2.1), as it requires no exhaust dust or other special accessories. The FDM head (Fig. 2.2) has two nozzles. One for model material and another for support material. Two different nozzles of hole diameters 0.305 and 0.635 mm are available, which can be changed as per the requirement. The liquefier in the head, melts the material at the temperature of 270° C for model material and 265° C for support material. The model is built in a closed cabinet maintained at 70° C.

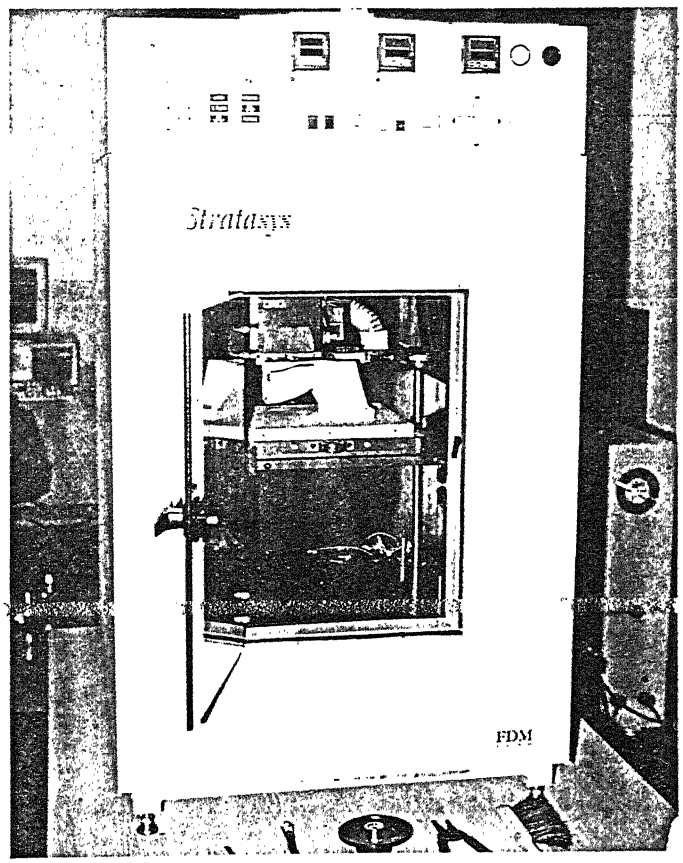

Fig. 2.1: The FDM1650 Machine

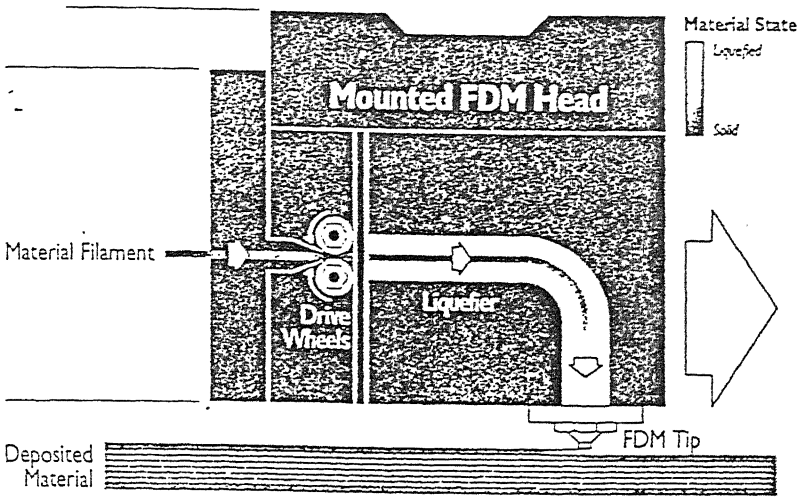

Fig. 2.2: Head of FDM1650

The head is mounted on a carriage which moves in x and y direction. The z movement is given to Z-stage platen. The model rests on the foam foundation provided on Z-stage platen. Both the model and support materials come in a wire form, from two different material spools located at the rear of the machine. On the front panel all the control buttons are provided to set the machine as per requirement. The controls such as x, y, z movement, temperature control, loading and unloading of material, etc. are available.

To run the FDM machine, first the nozzle tip of the required diameter is fitted on the head and the machine is cleaned. After sending the SML (Stratasys Machine Language) file, the initial x, y, z position of modeler tip is set properly with respect to foundation foam and the FDM machine is allowed to run. The head movement and material flow information for each slice curve is downloaded to the FDM1650. The FDM head deposits material as it follows the part geometry for each curve. For each layer, the head first deposits a perimeter road, which follows the shape of a slice curve, as shown in Fig.2.3. After the perimeter road, the head follows fill roads which fill the solid areas inside the part. When a layer is deposited completely, the platform is lowered by the amount of slice thickness and the process is repeated.

The FDM1650 features the Break Away Support System (BASS), allowing the designer to create models with greater speed and precision. BASS uses a second nozzle to extrude the support material. The supports are designed to prop-up the

overhanging portions of the part during modeling. The head automatically extrudes the support tip out wherever required. The supports detach easily, making the finished product look better with minimal post-modeling finishing.

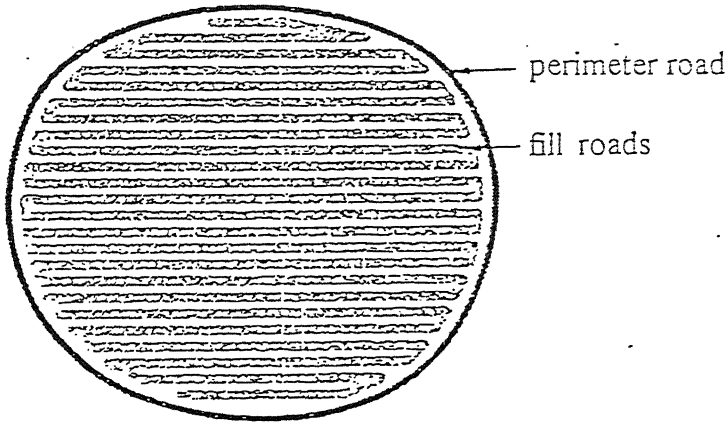

Fig.2.3: Perimeter and Fill pattern for each layer

2.2.3 Model Material

The FDM1650 is capable of using inert, nontoxic materials such as Investment Casting Wax and P400 Plastic (ABS Plastic). In the present work, P400 plastic is used for model making as it is a tough plastic which produces sturdy prototypes. P400 plastic is an Acrylonitrile Butadine Styrene (ABS) based material having the properties given in Table-2.1 .

Tensile Strength	34.5 Mpa
Flexural Strength	65.5 Mpa
Tensile Modulus	2482.8 Mpa
Flexural Modulus	2620.7 Mpa
Melting Point	270° C
Softening Point	104.4° C
Specific Gravity	1.05 gm/cc

Table-2.1 : Properties of P400 - ABS Plastic

The material comes wound on a spool in the form of a filament approximately 1.8 mm in diameter, so it is both easy to load and easy to store. The material change-over for Stratasys system is relatively quick and simple, with little material waste.

2.3 PROCESS PARAMETERS

The process parameters such as part orientation, slice thickness and attributes of slice curve influence the surface finish, accuracy and the time taken by FDM to complete the prototype. These are separately discussed below.

2.3.1 Part Orientation

The designer's choice of part orientation has an impact on build time, part resolution, surface finish, support structures, distortion, roundness, flatness, part tolerance, material cost, etc. All these attributes contribute to various degrees to the quality of the final product and have to be considered to have preferred orientation, which will require minimum running time, minimum support structure and give good surface finish. Minimizing the height of the geometry in z-axis will reduce the number of layers required, thereby decreasing the build time; but it may give rough surfaces, e.g. a long cylinder. For good surface finish, the part orientation should be selected which will reduce the stairstep effect (Fig.2.4 (a)). Fig.2.4(b) shows how stairstep effect can be avoided by a proper choice of orientation .

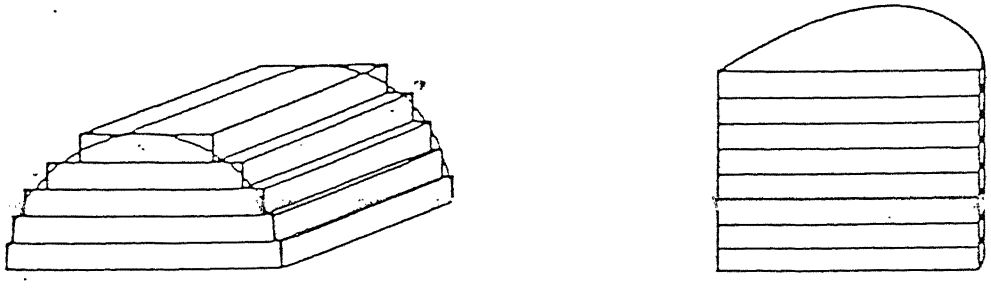

(a) (b)

Fig. 2.4: Effect of part orientation on surface finish

2.3.2 Layer (Slice) Thickness

The thickness of each slice of the part affects the surface texture and the accuracy in the *z*-axis. Layer thickness is one of the most widely used variables in rapid prototyping. As dimensions in the slice axis are rounded-off in increments of the layer thickness, one should carefully assess the selection of layer thickness. FDM1650 gives slice thickness of 0.178, 0.254 and 0.356 mm. More the slice thickness, lesser will be the running time, but that will also degrade the surface finish. In the present work, models with slice thickness of 0.254 are used. For this slice thickness, the nozzle tip of 0.305 mm is used.

2.3.3 Attributes of Slice Curve

When the FDM hardware builds a physical model, it lays down tracks of plastic called "roads". These roads follow the shape of slice curves. The selection of attributes such as road width, road height (slice thickness) and fill patterns (Fig.2.3) is dependent on the part accuracy and part building time. The part will be more accurate, if the road width and the road height is minimum, but then it will take more time to build the model. Increasing the road width, increases the pores in the model. The default value for road width of 0.508 mm is used for making the prototypes.

2.4 SOLID GROUND CURING

This system is a liquid rapid prototyping (Fig. 2.5) system by Cubital Inc., Israel. It is called as a *liquid rapid prototyping* system because it uses a liquid photosensitive (Ultra Violet Curable) resin to make the component. It uses the solid ground curing technology to make the prototype [6]. The process is based on instant, simultaneous curing of whole cross sectional layer area as a result of which its speed is about eight times faster than the other rapid prototyping systems. Solider systems offer real flexibility in production volume layout and size. The SGC technology allows the models to be nested freely and placed in any orientation. The surface finish obtained in this process is much better than other processes. Porosity is very less in these models as each layer is made in a single shot and the whole layer is a solid unlike the SLA and FDM processes. As the models have less porosity these are more amenable to mold making. The total process is divided into two stages (Fig. 2.6).

(a) Model preparation. (using Data Front End [DFE] software)

(b) Model production. (using Model Production Machine [MPM])

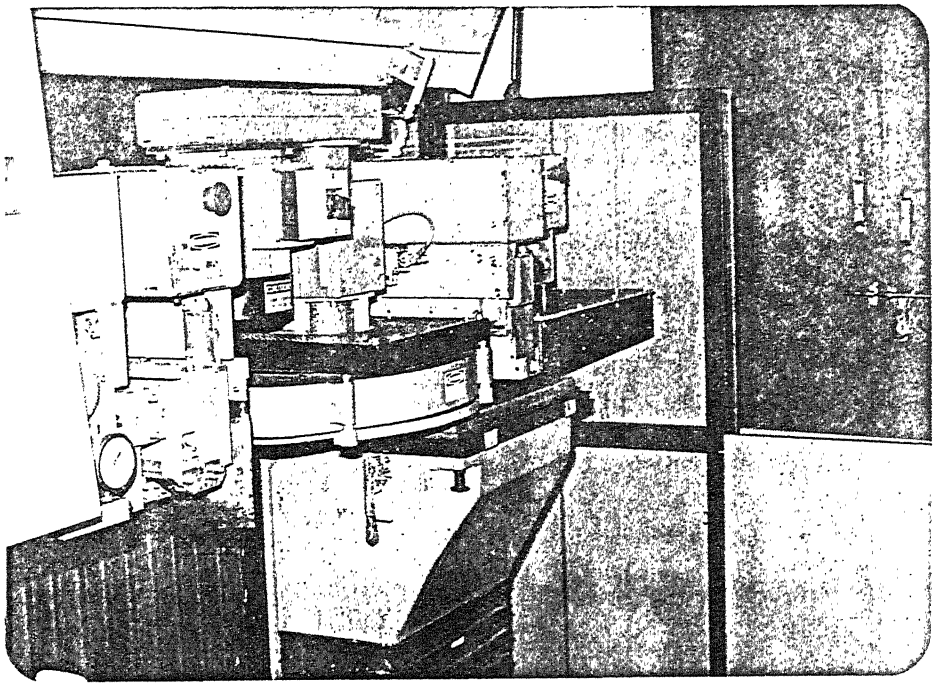

Fig. 2.5 SOLIDER 4600

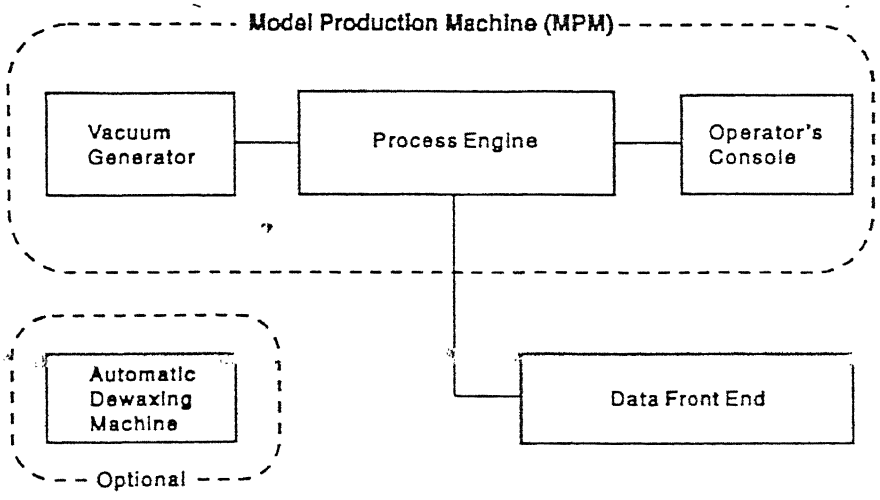

Figure A-1. Solider 5600 System block diagram

Fig. 2.6 Solider Block Diagram

2.4.1 MODEL PREPARATION

The model preparation is through the graphical user interface provided by Cubital Inc., through the DFE (Data Front End) software. The different input file formats for the DFE software include STL(Binary & Ascii) and CFL(Cubital Facet List) formats.

The DFE software uses a SOLI file format for internal communication between different stages of the software. The SOLI file is used in the DFE software as it occupies less memory as compared to other file formats. SOLI file uses polygonal facets to represent the outer shell of the solid model.

The DFE software includes a number of model editing and file conditioning tools and is divided into four easy-to-use software modules. It includes (a) Reception (b)Academy (c) Show (d) Production. DFE uses a Theatre analogy to describe the process of preparing objects for a production run. The objects in the production run are the "ACTORS" in the show and the Solider workbench is referred to as the "STAGE".

2.4.2 RECEPTION

Reception is used to import 3D part data in industry standard file formats and converts it into a SOLI file used for processing within the DFE software. The import file should not contain any redundant data and it should not have any flaws. If there are any unacceptable physical characteristics like incorrect facet dimensions or missing facets the input file will not be converted into a SOLI file.

2.4.3 ACADEMY

Academy is a Solider DFE application that enables one to improve an actor's physical characteristics and repair the possible flaws in the SOLI file. Academy has four characteristics.

Interfacing: Introducing the actor into the academy and getting the information on its history and current state.

Editing: It involves geometric transformation (rotation and scaling), model cutting widening and separation of actor items.

Corrections: It includes binding of nearby borders between two items or patching

gaps in items.

Compression: It involves reducing the size of the data required to represent the actor either by uniting facets that are on the same plane, or by uniting nearby vertices.

2.4.4 SHOW

It collects and organizes a group of actors for a production run on the MPM. The following design goals can be met in SHOW.

a) Maximum number of actors can be placed in minimum height and volume by fitting them together efficiently as shown in Fig. 2.7

b) The surface quality can be optimized by orienting the walls and other major surfaces of the model parallel to the primary axes of the show volume.

c) It allows creation of complex structures, such as models or casting molds, by combining number of actors into compound assemblies.

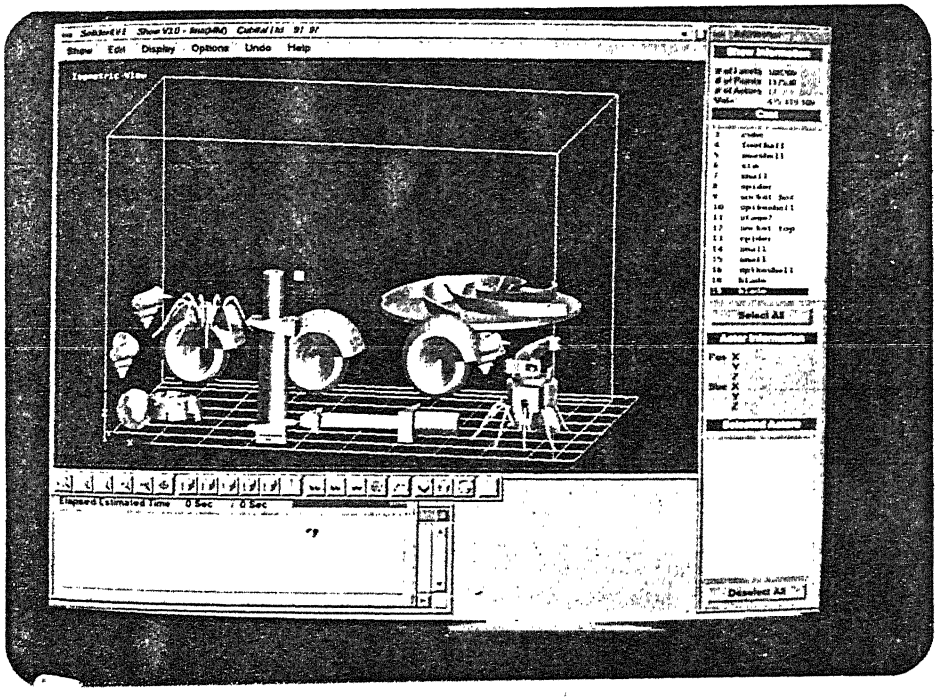

Fig. 2.7 Nesting of actors in SHOW

2.4.5 PRODUCTION

This application of DFE allows two major operations.

1) **Preview:** The production file to determine if any actors need to be modified or repositioned.

2) **Submit:** This is used to submit the production file to the MPM for production. The data for each layer is stored in a separate file called a CDT(Cubital Data Transfer) file and this is sent to the machine.

2.5 MODEL PRODUCTION MACHINE

The total process of making the model, once the layer data is sent to the machine includes two cycles. The first cycle is the *Mask Generation cycle* and the second cycle is the *Model building cycle.* The various functional units in these two processes are explained below.

2.5.1 MASK GENERATOR CYCLE

The entire Mask Generator Cycle is monitored and controlled by the internal computer called the Process Controller. The cycle begins and ends with the Mask Frame underneath the Primary UV Station where a generated mask is positioned above a layer of liquid resin spread on the Model Tray.

The steps in the cycle are (Fig. 2.8):

a. Layer of resin is exposed to UV light.
UV light passes through the transparent areas of the mask, and hardens the resin underneath.

b. Mask removed.
After exposure, the mask Frame moves left to the Toner Unit. While in motion, a rubber blade wipes toner off the Mylar sheet and collects it for re-use. The Mask Frame moves to the Ionographic Unit where electrostatic charge is neutralized by the Erase Rod. The Mask Frame moves to its extreme left position and stops. There it waits to produce the next mask.

c. Residual charge discharged.
The Mask Frame moves right to the Ionographic Unit where electrostatic charge is neutralized by the Erase Rod.

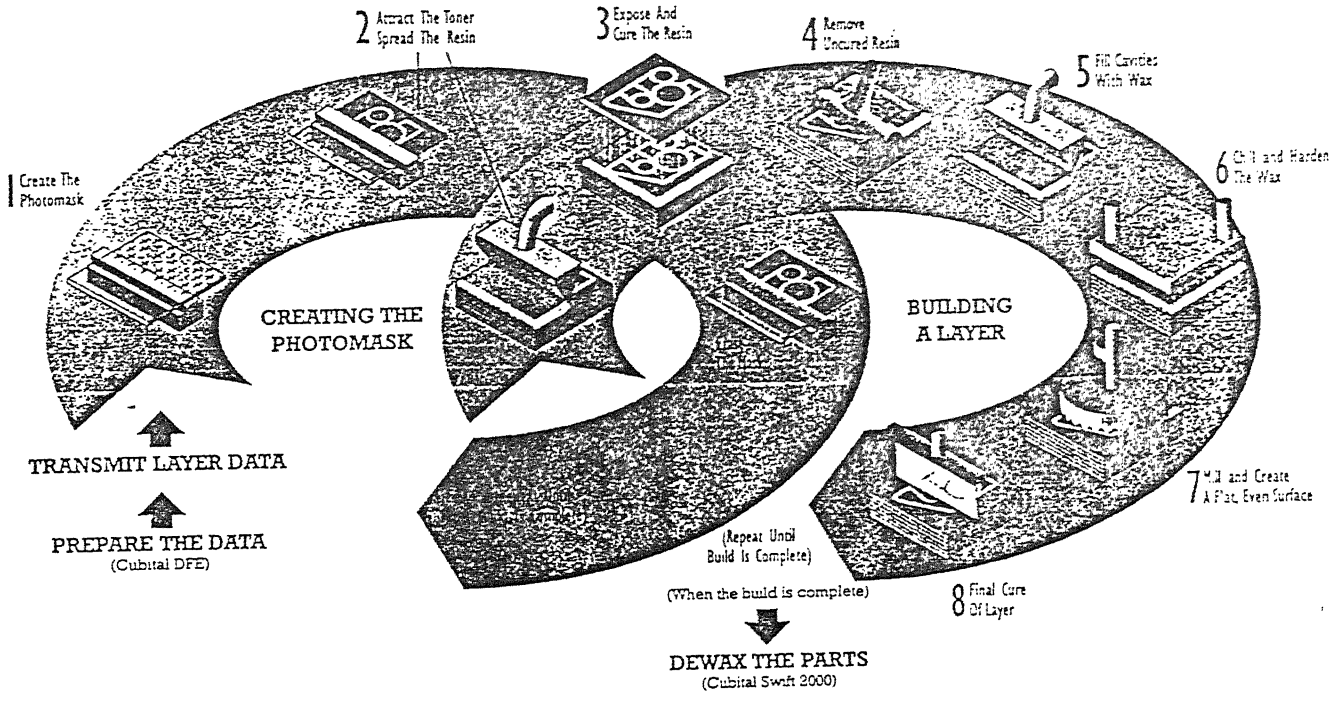

Fig. 2. 8 The Solid Ground Curing process.

d. Generation of a latent image pattern.

The Ionographic Unit places electrostatic charge on areas of the Mylar sheet that are to attract the toner. The shape of these areas is determined by the data received from the Process controller.

e. Mask produced.

The Mask Frame with the charged Mylar Sheet moves to the Toner Station. Toner is attracted to the charged areas of the mask.

2.5.2 FUNCTIONAL UNITS

Fuctional units consists of the following units (Fig. 2.9)

a) Motion Unit: The Motion Unit moves the mask from one station to another. It mainly consists of mask supporting frame, motion track and horizontal motion drive. The mask is supported by the mask supporting frame which is guided through the motion track and driven by the horizontal motion drive.

b) Mask Unit: The mask determines the geometrical shape of the next layer added to the model. The components making up the Mask Unit are described below. The mask unit consists of a mylar sheet and a metal coated glass. Mylar sheet is a transparent sheet on which the mask is generated which stores electrostatic charge that

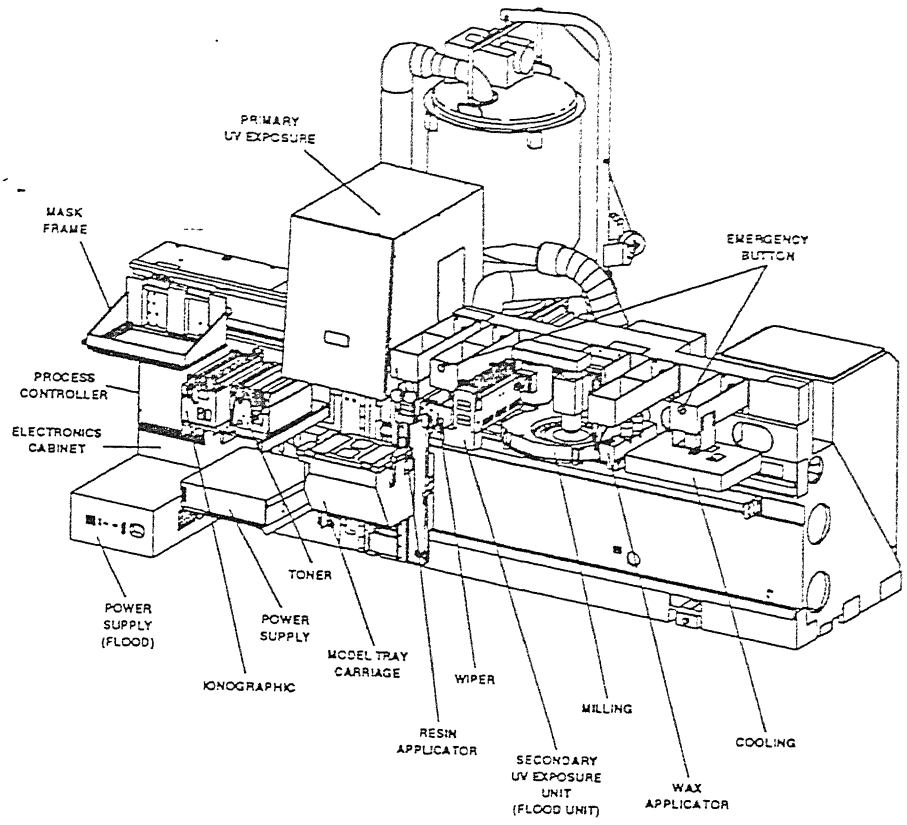

(a) Front View

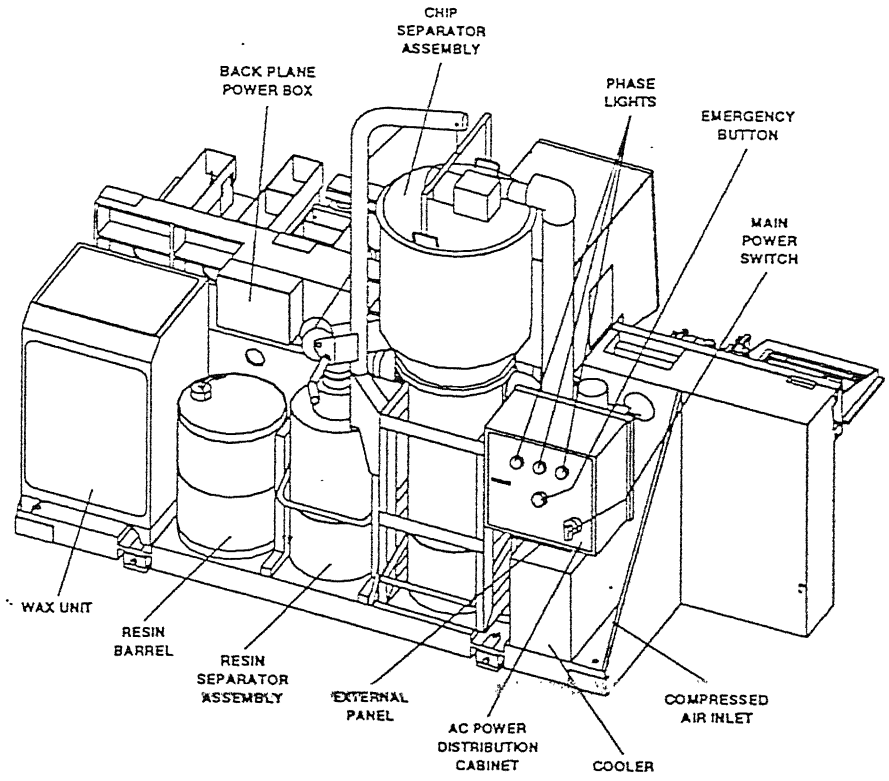

(b) Back View

Fig. 2.9 Model Production Machine

attracts toner to generate the mask. This sheet of non-conducting plastic material is glued over the Metal-Coated Glass, which stabilizes the position of the electrostatic charge placed on the Mylar Sheet.

c) **Ionographic Unit.** The Ionographic Unit neutralizes charges from the Mask Unit and creates an electrostatic image of the next layer on the Mylar Sheet. The major components are:

Erase Rod. It discharges the residual charge from the Mylar sheet. There are six axial wires on the circumference of the cylindrical rod. Among these one is active and the other five are idle and are used as spares.

Ion Cartridge. It jets ions into the Mylar sheet creating an electrostatic image of the next layer. The upper surface of the cartridge contains holes(256 angled rows of 16 holes each) that are fired in a pattern determined by the information received from the Process Controller.

d) **Toner Unit.**

The toner unit removes the previous mask and develops the next one. After primary exposure, the toner unit wipes toner from the Mylar Sheet thereby erasing the previous mask. After the next electrostatic image is formed on the sheet, toner from the Developer Unit is attracted to the charge areas, creating the mask for the next layer.

2.5.3 MODEL BUILDER

The model builder produces a three dimensional model layer by layer. The shape of each layer is determined by a mask generated for that layer. The entire model building cycle is monitored and controlled by the process controller. Th cycle begins and ends at the resin station where a new layer of resin is added. Except during UV exposure, the processing is carried out while the model tray is moving underneath the functional units. The steps in adding a new layer to the model are

1) Layer of resin is added to the model at the resin station. A thin layer of liquid resin is applied.

2) This layer of resin is exposed to UV light at the primary UV station. Model tray moves to the primary UV station. The mask, located between the UV light and the model tray, is already prepared with toner to define the shape of the layer. Then UV light passes through the transparent areas of the mask and hardens the resin underneath.
3) After the resin is cured at the UV station uncured resin is removed at the wiper station. An aerodynamic wiper plate creates a strong air jet that lifts off the uncured liquid resin. A suction slit removes the lifted resin, revealing the wax in the model.
4) The remaining resin is cured at the UV station in the secondary exposure. UV light floods the layer to complete the hardening of the resin representing solid areas in the layer.
5) After the resin is taken through the secondary exposure a layer of wax is added to the model at the wax station. A layer of melted wax, that covers the cured resin and fills voids, is then applied with the wax applicator.
6) Wax layer is then solidified at the cooling station. A metal plate cooled by water chilled to 4°C presses down on the wax layer and solidifies it.
7) A new layer is milled to the specified thickness at the milling station. Rotating diamond tipped blades mill away excess wax and resin to leave a new layer at the specified thickness.

The model building cycle starts again to produce a next layer. A typical cycle takes 100 seconds to complete a layer.

2.5.4 FUNCTIONAL UNITS (MODEL BUILDING CYCLE)

The various functional units in the model building cycle are discussed here under (Fig. 2.9).

(a) Resin unit. The resin unit covers the entire upper surface of the Model Tray with a uniform layer of liquid resin. The thickness is adjusted to 160-220 μm in height. The resin unit pumps liquid resin from a storage barrel into the applicator. In the applicator the resin is heated to the required temperature to maintain the viscosity of the resin at a particular value before spreading on the table. The viscosity should not change throughout the process because with the change in viscosity of the resin

the thickness of the layer formed on the table changes. For a particular thickness of the layer the exposure time is set to a particular value which depends on the resin properties. With the variation in the viscosity of the resin due to environmental influences the thickness of the resin spread on the table changes.

(b) **Primary Exposure unit.** The primary UV unit selectively polymerizes the resin layer by exposure to UV radiation through the mask. The exposed portions of the resin are polymerized and remain on the workpiece when the unpolymerized liquid resin is removed by the wiping unit.

UV lamp. A quartz bulb is located in a reflector cavity which receives energy from a magnetron that generates microwave energy at 2450 MHz. The microwaves heat the bulb to create a radiation-emitting plasma. The spectral characteristics of the emitted radiation are controlled by chemical additives in the bulb. Protective screens prevent microwave radiation from escaping to the surrounding area. An igniter bulb is included in the system to ensure proper starting of the lamp bulb.

Shutter. It is a pneumatically operated system to control the exposure time of the resin to UV radiation.

Magnetron cooling interlock. It shuts down the system if magnetron heats up beyond operating temperature. When the magnetron cools down, the system resets automatically and operation can resume.

(c) Wiping unit.

The wiping unit removes liquid resin from the top surface of the model. The liquid resin left represents 'spaces' in the model layer. The major units of the wiping unit are

Air blower and slit. It produces a thin, powerful stream of air to lift liquid from the surface and to roll the wave of liquid resin towards the collector collector blade and slit. An air pressure gauge and regulator are used to maintain the correct air supply for the blower.

Collector blade and suction slit. It guides the rolling wave of liquid resin into the opening of the slit. The vacuum presure present at the slit opening

extracts the liquid resin from the blade and carries the resin into the resin separator.

Resin separator. It separates the liquid resin from the air stream to collect it for reuse and to prevent it from reaching the vacuum unit.

(c) Wax Unit.

After the liquid resin remaining from the primary exposure is wiped away, the wax unit spreads a layer of liquid wax approximately 300 μm thick across the entire surface of the model tray. The wax covers hardened resin and fills in void to support the structure of the models during model building cycle. The wax unit

- Melts blocks of wax in the melter
- Stores melted wax and continuously stirs it in a conditioning tank
- Heats melted wax throughout the unit.
- Pumps melted wax from the conditioning tank into the applicator
- Lowers the applicator 2 mm downward to the spreading height, and after spreading, lifts it back to idle height
- Pushes a volume of melted wax through a slit and spreads it like a blanket onto the upper surface of model tray.

(e) Cooling unit:

The cooling unit rapidly cools and solidifies the wax layer. The cooling occurs by physical contact between the wax layer and the cooling plate. The cooling sequence is as follows

- After a liquid wax layer is spread, the model tray moves to underneath the cooling plate.
- The model tray it's position
- The piston moves the inner Box downward. When contact is made with the outer box, the inner box pushes the outer downward and chills the cooling plate.
- Both boxes move down and press together on the wax layer. The cooling plate chilled by the cold transfer plate, solidifies the wax.

(f) Milling unit:

The milling unit mills the layer of solid wax and hardened resin to a finished thickness of 150 ± µm. As the milling proceeds, the milling unit sucks chips and dust out of the milling area for disposal.

(g) Vacuum unit.

The vacuum unit used by the wiper and milling unit. The vacuum generator generates a strong vacuum using an electric motor which drives a large turbine. The vacuum manifold switches the vacuum source between the resin separator and the chip separator line.

2.6 PROCESS PARAMETERS IN SGC

a) Layer Thickness:

We can increase the thickness of the layer to decrease the time taken for the object to be manufactured. But with the increase in thickness the surface finish will be reduced due to the stair case effect. Besides this, if the thickness of the layer is increased so should the exposure time of the UV light. Due to increase in exposure time the UV light will pass through the mask covered by the toner particles and solidify the resin which is outside the required section.

b) Room Temperature

The room temperature greatly effects the quality of the model. If the room temperature is less than the prescribed value the viscosity of the polymer increases. Due to the increase in viscosity, the thickness of the layer formed on the table during spreading increases. But, as there is no corresponding change in the exposure time the energy supplied by the UV light is not sufficient to glue the present layer to the previous one. Due to the weak bonding, the layer is peeled off during wiping and wax is allowed to solidify in these vacated places. Ultimately in the final model, a wax layer is present between the two resin layers which reduces the strength of the model.

If the room temperature is higher than the prescribed value, the viscosity of the polymer decreases. So, the thickness of the layer formed during spreading decreases, which is less than the final thickness (150 microns) required. This gap

is filled with wax and ultimately the strength of the model decreases due to these wax inclusions.

C) Temperature of Water During Dewaxing

The temperature of the water used to dissolve the wax should be equal to the temperature prescribed, which is set based on expansion ratios given during model preparation. So, by changing the temperature of the water from the prescribed value, dimensional accuracy of the model will be effected.

2.7 MACHINE SPECIFICATIONS

- Gross working volume — 500x350x350 mm^3
- Dimensional accuracy of models
  - Typical — 0.5 mm
  - (measured between targets through the material in any direction)
- Model resolution :
  - X-Y resolution — 0.1mm
  - Z resolution — 0.1 – 0.15 mm
- Minimum feature size:
  - Typical — 0.4 mm
  - Horizontal plane — 0.15 mm
  - Vertical plane — 0.6mm
- Gross production rate — $1.181x10^6$ mm^3/hr
- Model pre-processing time — 20 min to 3hr
- Model post-processing time — 30 min to 3hr

2.8 SOLIDER MATERIALS

Solider resins are Acrylic based photopolymers specially formulated for use in the Solider model production process. The resins are non-volatile and insoluble in water. Polymerization may be initiated by heat, oxidizing agents, or exposure to UV radiation. The resins are supplied with a polymerization inhibitor which have limited life-time of six months. There are two kind of resins namely G-5601 and X-607 for making the models. The turbine blade model used in the present work was made of

G-5601. The properties of the material are:

Liquid resin

1) Density	@ 25°C	1080 kg/m3
2) Viscosity	@ 20° C	6500 m Pa s
	@ 30° C	2300 m Pa s
	@ 40° C	900 m Pa s

Cured Resin

1) Tensile strength	@25° C, 50% RH	30 Mpa
2)Elongation	@ 25° C, 50% RH	15%

2.9 PARTS BUILT FOR THE PRESENT WORK

The list of the parts built on FDM1650 machine, the SOLIDER machine and the MCP-Vacuum casting machine for experimental purpose is given in Table-2.3 and Fig. 2.10 shows the parts made in the FDM and SGC process.

Sr. No.	Prototype/Method	Dimensions (mm)	Slice thickness (mm)	Build Time (hrs)	Qty.
1	Circular Disc/RT	ϕ 60 x 6	0.254	-----	7
2	Turbine Blade/Solider	------	0.150	5.5/part	2
3	Turbine Blade/FDM	——	0.254	11.2/part	1
4	Turbine Blade /RT	-----	-----	----	6

Table-2.3 Parts Built for the present work

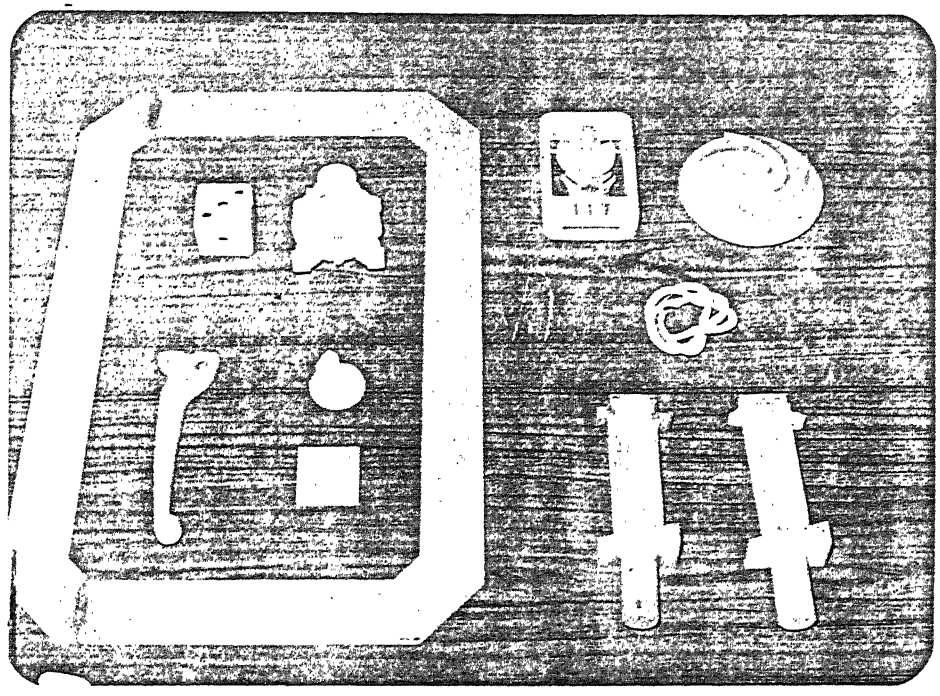

Fig 2.10 Models made on Solider 4600

Chapter 3

RAPID TOOLING

3.1 INTRODUCTION

Although RP was introduced as designers visualization tool, the cost involved does not justify its usage restricted to visualization alone. This has given way to the evolution of the RAPID TOOLING (RT) technology. Rapid tooling is a technology that adopts Rapid Prototyping (RP) techniques and applies them to tool and die making, is becoming an increasingly attractive alternative to traditional machining. The move from traditional machining methods to RT is more a leap than a step.

When effectively implemented within a concurrent engineering environment, RT has the potential to dramatically improve the speed and cost of product development. Using Computer-aided design, electronic data transfer, process simulation, and RT technologies, tooling costs and development times can be reduced by 75 percent or more [7]. RT is useful when tool geometry makes traditional machining difficult because of part complexity or specific geometric features such as undercuts. In this work the main area of concentration has been the establishment of a new technique by the fusion of RP, RT and Digital Photoelasticity techniques, to stress analysis of complex components like turbine blade. The MCP Vacuum Casting machine of HEK GmbH, GERMANY has been used for making the mold and the models.

3.2 CLASSIFICATION OF RAPID TOOLING

There are several ways in which the tooling can be manufactured rapidly. These are classified into the following two major groups.

(a) Indirect RT processes

In these processes the starting point is the Rapid Prototype of the component for which the tooling is to be manufactured. The MCP Vacuum Casting process is an indirect RT process in that it needs an RP model for making the component.

(b)Direct Processes

In these processes the tool is directly manufactured in layers. From the CAD data available the mold can be designed for a particular component and the resulting mold can be made by any RP process.

3.3 MCP-VACUUM CASTING MACHINE:

The MCP Vacuum casting machine is shown in Fig. 3.1. It has two chambers the upper and the lower [8]. The upper portion of the chamber houses the stirrer motor assembly. It has three platforms to hold the cups A and B and the funnel through which the resin flows into the mold, placed in the lower mold chamber. All the resins used for casting the molds are available as two component resins. To control the mixing of these resins in the vacuum chamber there are different functions on the control panel of the vacuum casting machine. The control panel controls the rotations of the cups A and B and the motion of the stirrer. There is a facility to release the vacuum in a slow and a fast manner which is helpful in primary de-gassing and secondary de-gassing of the silicone rubber and in vacuum casting of the resins.

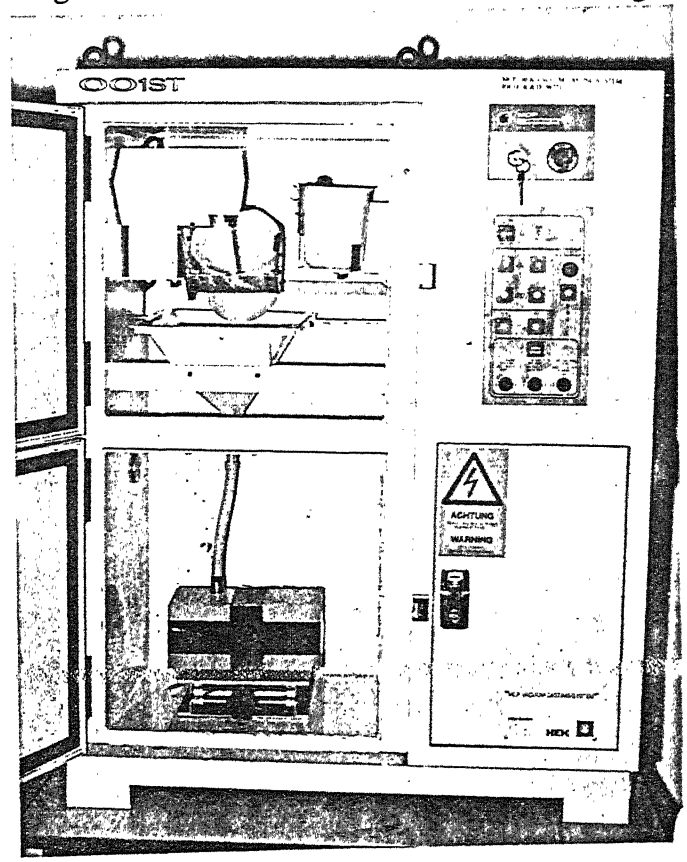

Fig. 3.1 MCP-Vacuum Casting Machine

The vacuum casting machine also requires ovens (Fig. 3.2) to cure the silicone rubber and the resins. The RTV 750 silicone rubber is cured in the oven at 40°C for 8 hrs. The resins are to be cured at a temperature of 70°C for a period of 40 mins. Two ovens are provided along with the MCP Vacuum casting machine, the temperature range of which is upto 140°C. In these ovens the temperature rise-rate is approximately 5°C/min when the ventilation slide of the oven is closed and it is 0.2-0.5°C when the ventilation slide of the oven is open.

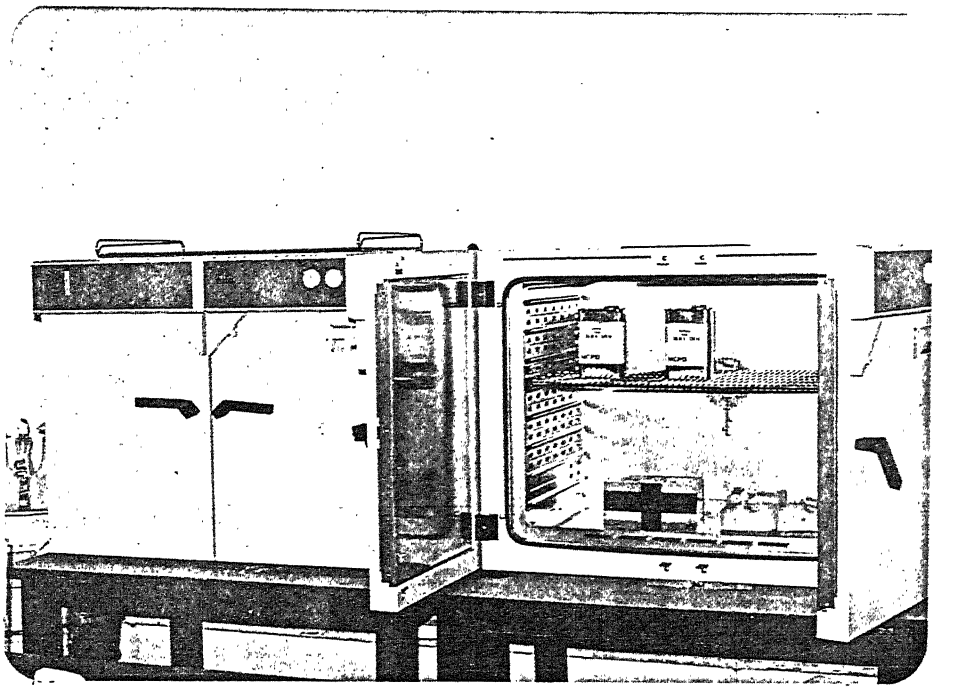

Fig. 3.2 The Curing Ovens

The maximum mold size that can be made from this machine is 400*400*320 mm. The vacuum that is developed in the chamber is 0.5 m bar.

3.4 VACUUM CASTING

3.4.1 PREPARATION OF THE MODEL

Silicone rubber is a polymer that reproduces the surface accuracies or the inaccuracies exactly. It has very good releasing properties. Sufficient care has to be

taken in preparing the specimen for making the mold. The components made from the FDM process have porosity which is detrimental to mold making in some cases. Silicone rubber enters these pores and it becomes very difficult to remove the component from the mold. Hence a lot of care is to be taken in preparing the component. The master model is to be thoroughly cleaned and if necessary an MCP barrier coat is to applied. Silicone rubber is flexible and can be easily cut with a knife that allows the models to have non-planar parting lines of any complexity. The parting line of the mold has to be decided carefully and care has to be taken to avoid any deep undercuts.

3.4..2 CASTING A MOLD IN SILICONE RUBBER

The whole of process of making the mold includes the following steps.

a) MARKING & GATING

Apply clear marking tape at the parting line and color the edge of the tape with a marker pen as shown in Fig. 3.3 (a) and Fig. 3.3 (b) to assist in cutting the mould into two halves. The correct size and number of gates depends on the size, shape and weight of the component. Multiple gates give better castings. After taping the model, the gates are formed by gluing rods of ABS, nylon or metal. The diameter of the gates should be 10, 15 or 20mm, as needed to match the hose connectors.

b) CASTING FRAME

The casting frame can be made of wood, ABS or laminated chipboard. The size of the mold is arbitrary. In general if the component is of dimension X*Y*Z the molding frame is of (X+60)*(Y+60)*(Z+90). The extra height on the frame is needed to contain the silicone rubber during the secondary de-gassing operation. On the larger molds the dimensions of the frame are to be increased proportionately. The model is supported in the casting frame by using supports as shown in the Fig. 3.3 (c).

c) SILICONE RUBBER CALCULATIONS.

The weight of the rubber needed is calculated by calculating the cubic capacity of the finished mold. The cubic capacity multiplied by the specific gravity of the rubber

(1.1) is calculated to give the weight of the rubber needed. The mold height should be taken as being approximately 30mm above the highest point of the model, and not to the top of the casting frame. The amount of catalyst needed is 10 % by weight of the rubber. The rubber is to be taken in a container of capacity approximately five times greater than the amount of rubber to accommodate for the increase in the volume of the rubber during de-gassing. After adding the catalyst the rubber is to be mixed thoroughly for minutes to ensure uniform mixing. Once the catalyst is mixed the whole process of poring the rubber is to be completed within seventy minutes.

d) PRIMARY DE-GASSING

The container having the rubber is placed in the vacuum chamber and a vacuum of 20 Torr is applied for ten minutes. As the volume of the silicone rubber will increase while primary de-gassing this process is to be carefully followed lest the silicone would overflow. If the level of the rubber is increasing and reaching the top of the frame the FAST LEAK control button should be pressed once or twice to reduce the level in the container.

d) POURING THE RUBBER.

After primary de-gassing, the liquid is poured slowly (Fig. 3.3 (d)) and steadily into the casting frame. The rubber must first be allowed to flow under the bottom of the model to avoid any disturbance in the model. The time for primary de-gassing should be kept as low as possible as the flowability of the silicone rubber decreases with time. It would be very difficult for the rubber to flow and fill the whole volume if its flowability decreases. The rubber has to be poured very carefully, avoiding any sudden rush of rubber into the mold.

e) SECONDARY DE-GASSING.

Place the mold in the vacuum chamber and carry out the same procedure as described above in step 4 (Fig. 3.1).

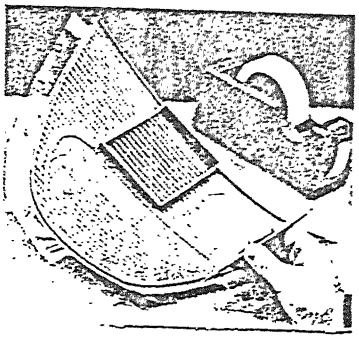

(a)

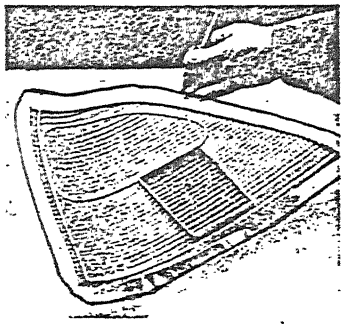

(b)

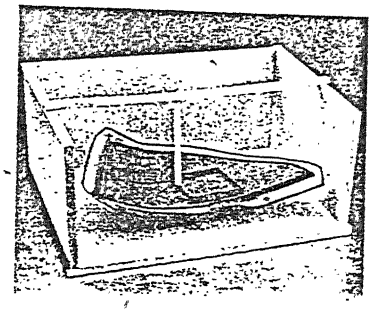

(c)

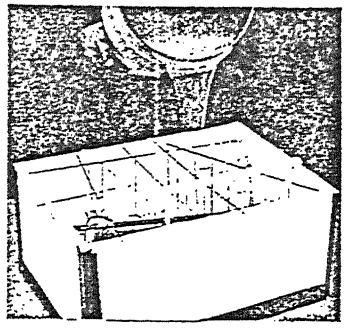

(d)

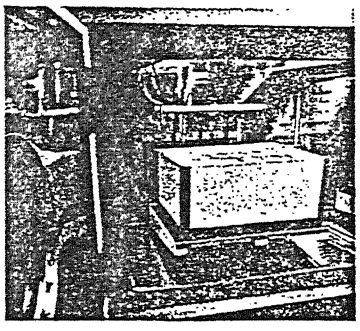

(e)

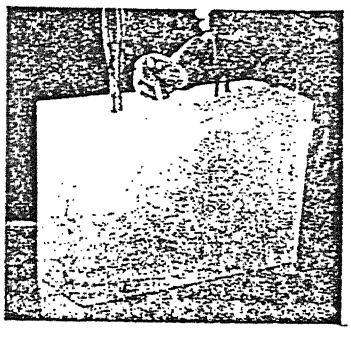

(f)

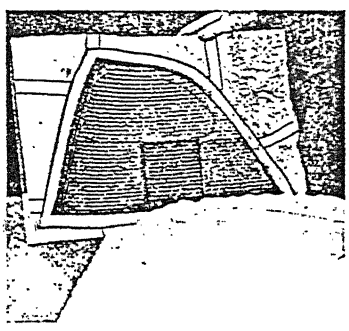

(g)

Fig. 3.3 The Mold Making process

f) CURING THE MOLD.

Although silicone rubber may be left to cure (Fig. 3.3 (e)) at room temperature for 12 hrs, it is recommended that, for extreme dimensional accuracy in the castings, the rubber is cured in an oven at 40 °C for atleast 6-8hrs.

g) SEPARATING THE MOLD.

When the mold is fully cured, the casting frame is removed and the venting and gating rods are removed. As the mold is transparent the component and the parting tape marked dark can be easily seen through the mold (Fig. 3.3 (f) and Fig. 3.3 (g)). Some typical molds made in the vacuum casting system are as shown in the Fig.3.4. The mold for turbine blade can also be seen in the figure. To help identify the correct line while cutting, a dark line is drawn on the mold following the contour of the contour of the taped split lines. With the help of special tools like the mold openers and knives the mold is cut open. The cut is to be made only upto the marking tape. Thuswise it is ensured that the mold areas are not damaged under any circumstance. The cut is made in a wavy fashion to ensure a perfect fit between the mating parts. After cutting the mold is ready for resin casting.

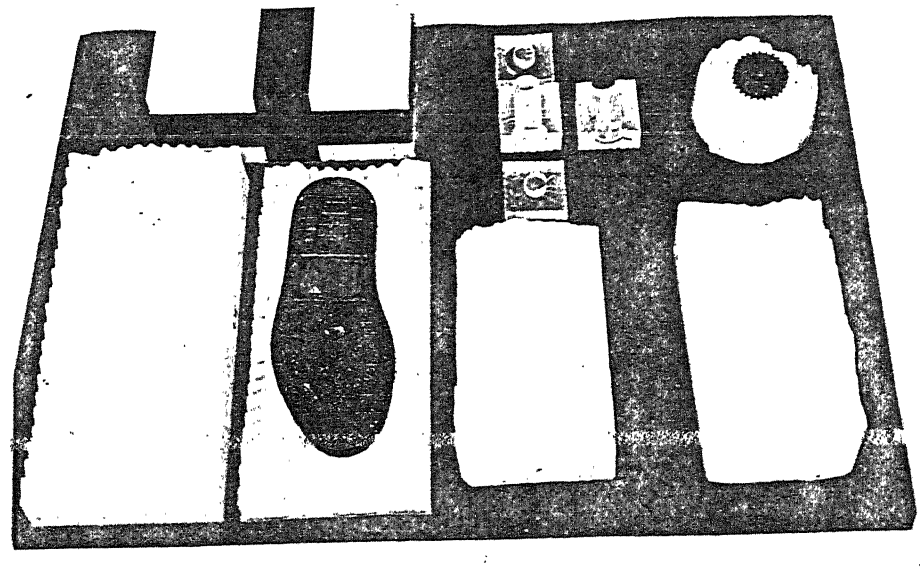

Fig. 3.4. Molds made in the Vacuum Casting Machine

3.4.3 RESIN HANDLING AND PREPARATION.

The resins that are available for casting from HEK GERMANY are in two parts namely resin A and resin B. The component 'B' is liable to crystalline at low ambient temperatures. Ideally, both resin components (A and B) should be stored at about 25°C. These resins being hygroscopic in nature absorb moisture and hence are not be left open for longer times. If the resin gets crystallized the resin has to be heated to a temperature of 65-70°C for a period of two hours. If any signs of excessive crystallization are seen the time must be extended to 4 hours. After this step the resins are to be kept in a vacuum chamber for two hours. Degassing is completed when there are no more bubbles seen in the container.

The amount of resin required is to be determined by calculating the volume occupied by the master model (approximate) and multiplying it with the specific gravity of the resin. But some other allowances are to be provided to the resin to account for the resin that remains in the gating, vents, tubing, funnel and resin pots. The resin that remains in the resin inserts after pouring is called "pot rest". The pot rests for various resins are to calibrated as it plays a crucial role in the ratio of which RESIN A and B are mixed. This is done by experimentation. The pot rest for SG95 A is 0.009 Kg and that of SG95 B is 0.011 Kg.

3.4.4 WEIGHING THE RESIN

Insert cup liners into both A and B cups. Depending on the resin, the ratio in which the two components are mixed is decided. Some precautions to be taken with the resins are that the resin B should never be shaken and it should never be poured back into the container if it is taken out. The required amount of the resin is taken in the respective cups. In general resin A is taken in cup A and resin B is taken in cup B. If the pigment is to be added to the resin then resin B is taken in cup A and resin A is taken in cup B, because the pigment reacts with the resin B. The temperature of the resin when placed in the vacuum chamber is to be 30-35°C.

3.4.5 VACUUM CASTING OF THE MODEL

a) PREPARING TO CAST

The mold has to be coated with the releasing agents so that the components are easily released. First the mold surface is coated with the releasing agent without the silicone and then with a releasing agent with silicone. These agents also help in increasing the life of the mold. The silicone rubber molds become brittle with time and turn yellowish in color. After the coating the mold is taped as shown in Fig. 3.5 (a). This is to ensure a tight joint. Then the mold is placed in the vacuum chamber and attached to the funnel by means of a flexible hose and hose connectors. The mold is to be placed at the correct height with the help a lift. The cups and the stirrer are to be placed in the correct position.

b) VACUUM CASTING

The vacuum casting machine is put on and the stirrer is started to run at maximum speed. Before starting the machine it is important to ensure that both the lower and upper doors of the system are closed, without which the system would be damaged. The stirring is to be carried on for a period of 20 minutes. After which the cup A is tilted by a little more than 90°. The resin in cup A is mixed with the resin in cup B. The time taken by the cup A to come to its lowest position is 7 seconds. After the cup A comes to this position the time for which the resin in cup A is allowed to flow is 10 seconds (Fig. 3.5. (b)). After a period of 10 seconds the cup A is raised. This time period is the one used at the time of calibration of the pot rest for the resins. After this the resins are allowed to mix for a period of 40 seconds for SG 95 resin which is used in the present work. The time period of mixing depends on the resin which again depends on the pot life of the resin. After mixing for 40 seconds the cup B which contains the mixture is tilted (Fig. 3.5. (c)) to pour the mixture in the funnel. Once the mold is filled up (Fig. 3.5. (d)) the resin begins to flow out through the riser. At this instant the vacuum is released and the cup B is raised. After the vacuum is released the mold is taken out and is put in an oven at 70°C for a period of 1hr. once the resin is cured the mold is removed from the vacuum chamber and the tape is removed. With the help of mold openers the mold is slowly opened without distorting the component (Fig. 3.5. (e)). Some of the components made on the Vacuum Casting Machine are as shown in the Fig. 3.6.

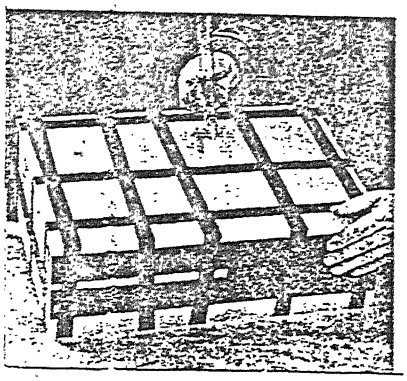

(a)

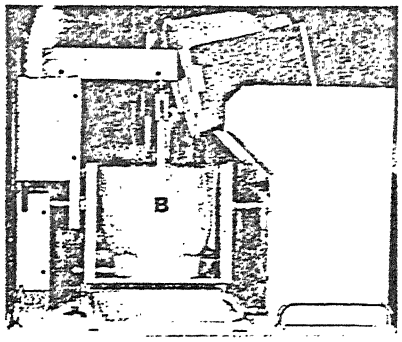

(b)

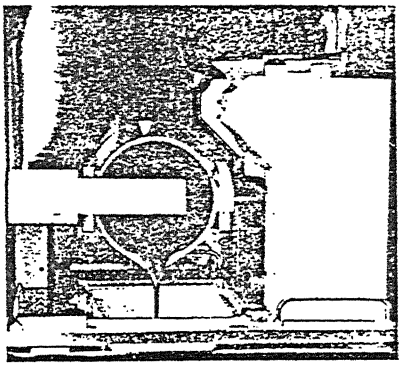

(c)

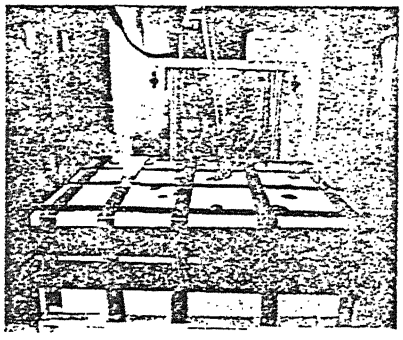

(d)

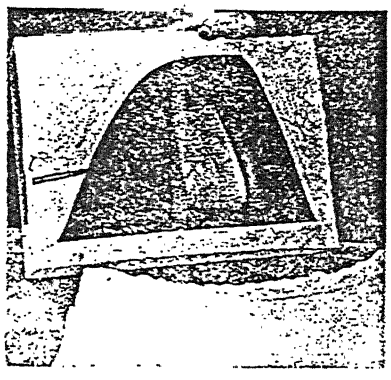

(e)

Fig. 3.5. Casting the Model

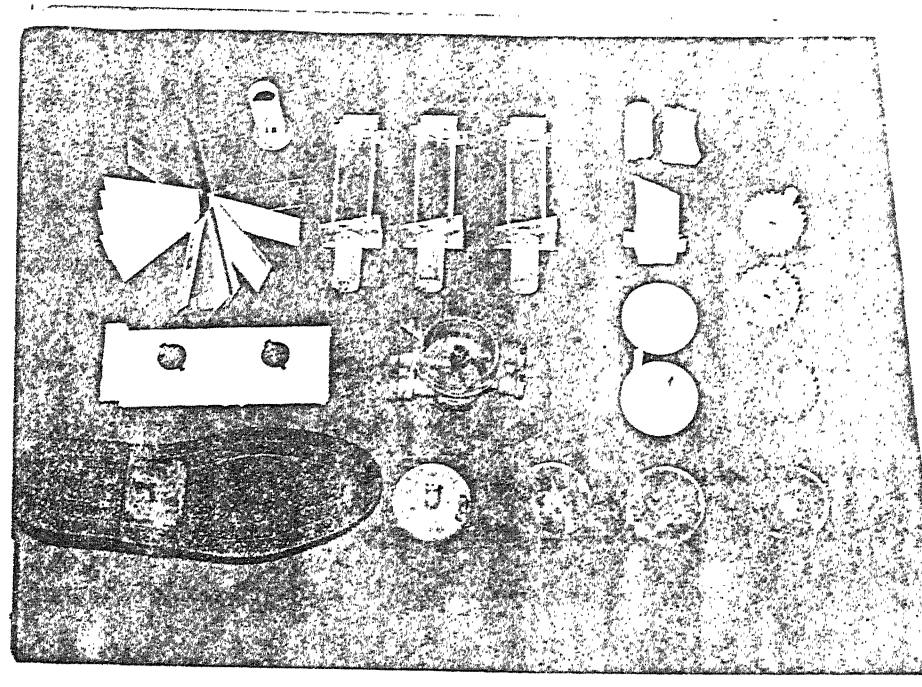

Fig. 3.6 Components made in the MCP Vacuum Casting Machine

3.5 VACUUM CASTING MATERIALS.

(a) Silicone Rubber.

Silicone rubber has silicone polymers in which silicon and oxygen atoms are linked together alternately. In addition two organic groups are connected to each silicone atom. One of the outstanding properties of the silicone rubber is its release action toward many materials. Some of the other properties include high molding accuracy, less shrinkage and heat stability. Because of the high flow and creep capabilities of silicone rubber even the smallest structures can be molded with exceptional accuracy. Surface defects up to 1µm in size can be reproduced with exceptional accuracy. The shrinkage of the silicone rubber depends on the amount of the catalyst added and is less than 0.1%. The silicone rubber used in the present research work is RTV (Room Temperature Vulcanisation) 750 rubber whose curing temperature is 40°C for a period of eight hours.

(b) Vacuum Casting Resins

The actual castings in this process are produced from specially formulated polyurethane resins. The resin is usually a two part mixture. Part 'A' is based on a polymeric hydroxyl compound or polyol (such as a polyester or polyol) with catalytic additives. While part 'B' is invariably a di-isocyanate of the type known as MDI. There are different varieties of resins provided by HEK GmbH that provide various combinations of hardness, toughness and flexibility. It is also possible to add coloring material to part 'A' (polyol) without affecting the quality of the final product.

The resin used for the photoelastic analysis of models is two component SG95 resin provided by HEK GmbH GERMANY. The ratio in which the two components of the resin SG 95 A and SG 95 B are mixed is 100:150. This resin is a photosensitive resin which contains poletherpolyols. The main component is a Polyoxypropylene glycerolether. It contains free MDI(4,4 - Diphenylmethane isocyanate) as the monomer. The isocyanate groups OCN of SG95 B react with the alcoholgroups OH of thePoluol of SG 95 A. The main component of SG 95 A has three functional groups. This means, that the end product contains long chains of polyol-isocyanate groups and in addition cross connections between these chains. Due to these cross-connections the polyurethane made from SG95 is a duroplastic and not a themosetting nor a thermoplastic one. The properties of this resin (SG 95) is shown in the table below.

Colour	Tranasparent
Mixing Ratio(A:B)	100 : 150
Specific Gravity (A) (B)	(1.07) (1.19)
Tensile Modulas(Mpa)	2521
Flexural Modulas (Mpa)	2195
Curing Temp	65°C - 70°C
Shrinkage	0.2%
Heat Deflection Temp.	72°C

Table-3.1 Properties of SG95 Resin

3.6 BETTER CASTINGS FROM SILICONE MOLDS.

The following points are to be taken care of in casting the component from the silicone molds.

1) The inside temperature of the mold should be 60°C and the heating cabinet should have a temperature of 70°C.
2) If the curing time is too short the castings would be soft, sticky and maximum temperature resistance is not reached. To avoid this the curing time should be in between 40 mins to 120 mins depending on the size of the component. At the same time if the curing time is too long the release agent dries off and the resin sticks to the mold.
3) High humidity can cause a lot of damage to the end components. If the humidity is high the resins are to be primary defoamed/degassed every 2-3 hrs. If possible the resins should be pre-heated to a temperature of 70°C and them de-gassed in the vacuum chamber. Materials which retain moisture, should never be placed in the vacuum chamber .
4) The gates and sprues should be of sufficient diameters. If they are too small the resin flows very slowly into the mold and causes early setting of the resin.
5) To avoid the bubbles which occur when the resins A and B are mixed together cast with the mold slightly slanting to allow the gases to rise to the highest points.
6) While casting as soon as the mold is filled the vacuum pump must be switched off and "slow leak" button is to be pressed and after a few seconds "fast leak" button is to be pressed. This is to release the vacuum gradually.
7) For transparent castings never use the release agents.
8) The following materials are not compatible to silicone and hence when used as master pattern, need to be sealed using the MCP barrier coat. The materials are PVC, non ferrous metals, clay, plasticine, SLA(Stereolithography models), oil based fillers and paint.

The Table-3.2 shown below gives a visual guide to the problems and their causes.

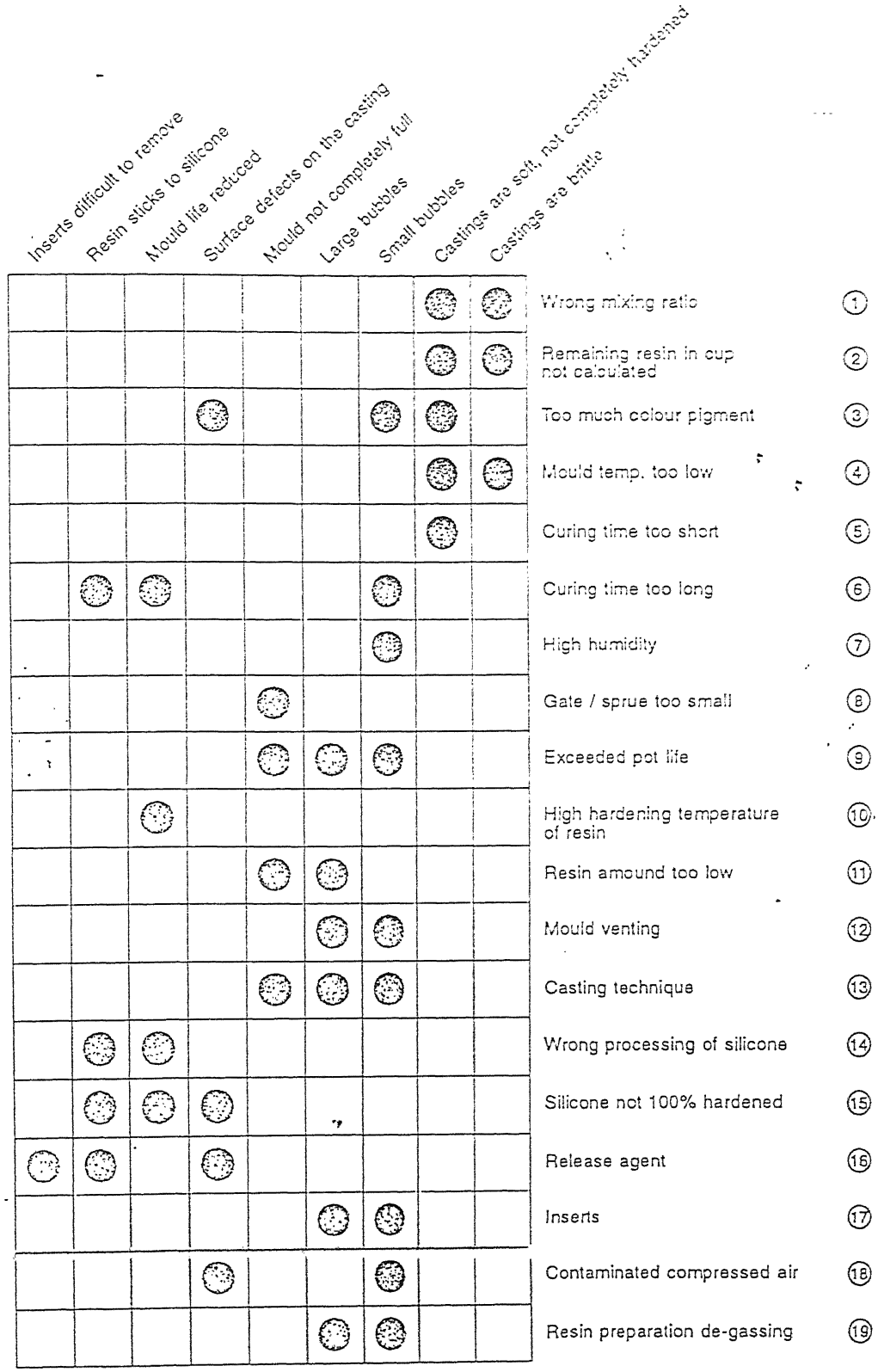

Table-3.2 Visual guide to problems and causes in castings

Chapter 4

PHOTOELASTIC ANALYSIS OF RT MODELS

4.1 INTRODUCTION

Component performance prediction by design analysis is a vital part of the development process and an area where RP and RT can play a vital role. The performance of many components is only verified by testing prototype parts, a stage that comes late in the development phase, leaving little time for amendments to be made to the design. Thus even at the design stage, the structural response needs to be studied. It is better that both numerical and experimental analysis is done before finalizing the design. In this chapter, the use of RP and RT for making three dimensional photoelastic models is investigated. The model materials are characterized by techniques of digital photoelasticty [9]. With the collaborative effort of CAD - Project Laboratories and Digital Photoelastic Stress Analysis Laboratories at the INDIAN INSTITUTE OF TECHNOLOGY, KANPUR an alternative approach to stress analysis is being developed by the integration of RP, RT and Digital Photoelastic techniques.

4.2 PRINCIPLE OF PHOTOELASTICITY

Photoelasticity is an experimental technique for analyzing stress fields in mechanics. It deals with the effects of stress and/or strain upon light. Certain noncrystalline materials, notably some polymeric plastics, are optically isotropic under normal conditions but become doubly refractive or birefringent when stressed. Like crystals, they then also have the ability to resolve an impinging light vector into orthogonal components and to transmit each with a different velocity. This effect normally persists while the loads are maintained but vanishes almost instantaneously or after some interval of time depending on the material and the conditions of loading,

when the loads are removed. This phenomenon was first observed by Brewester in 1816 and is the basic principle on which photoelasticity is based.

Within the past few years, development of RT technology and photoelastic resins made photoelastic testing of complex models very attractive. This is a significant breakthrough when a complete three-dimensional stress analysis of a design is required, since construction of the photoelastic test model by RP&RT is much faster and, in some cases, more economical than traditional photoelastic model-making (methods such as casting and machining). Photoelastic technique used to analyze 3D models is achieved by a process called *"stress-freezing"*, and slicing.

It permits a thorough analysis of the stresses throughout the volume of the model. Once measured, these stresses can be converted to equivalent levels that will exist in the actual part under similar loading conditions. Such detailed stress analysis on a physical test part is highly desirable for validating and refining finite-element methods.

4.3 POLARISCOPE

Polarization of the light is accomplished with a polariscope, the basic instrument used in photoelastic analysis. A simple plane polariscope arrangement, consisting of a light source, a polarizing filter, a transparent birefringent material, and an analyzer, is illustrated in Fig 4.1. The analyzer is identical to the polarizer except that its transmission axis is horizontal (perpendicular to the transmission axis of the polarizer).

The light source emits a train of waves containing vibrations in all perpendicular planes. However, the polarizing filter (Figure 4.1) transmits only one component of these vibrations (that which is parallel to the polarization axis of the filter). Such a beam is called plane polarized light because the vibration is contained in one plane.

In a plane polariscope one observes two sets of contours namely isochromatics and isoclinics superimposed over each other. Isochromatics represent the contours corresponding to principal stress difference and isoclinics represent the orientation of principal stress palnes. By using a circular polariscope one can make visible only the

isochromatics. Isochromatics are colored and a color sequence is available for determining the fringe order.

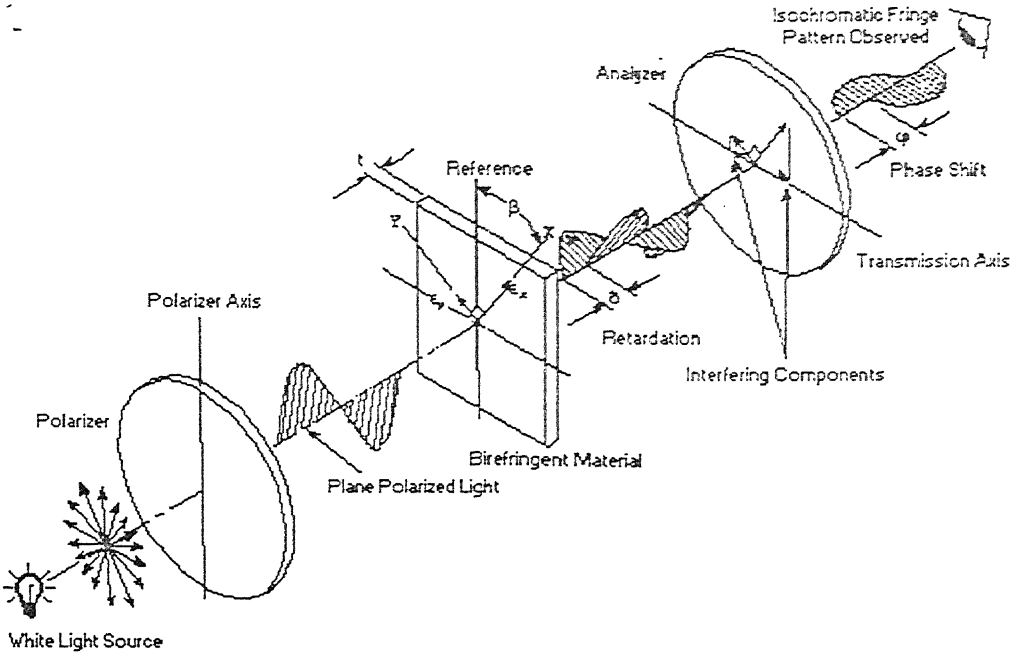

Fig. 4.1 Plane Polariscope

4.4 STRESS OPTIC LAW

The relations between stresses and the indices of refraction for temporary birefringent materials were formulated by Maxwell in 1852 as

$$n_1 - n = C_1 \sigma_1 + C_2(\sigma_2 + \sigma_3)$$
$$n_2 - n = C_1 \sigma_2 + C_2(\sigma_3 + \sigma_1)$$
$$n_3 - n = C_1 \sigma_3 + C_2(\sigma_1 + \sigma_2)$$

n = index of refraction of the unstressed material in its optically isotropic state

n_1, n_2, n_3 = principal indices of refraction for waves vibrating to the principal stresses

$\sigma_1, \sigma_2, \sigma_3$ = principal stresses

C_1, C_2 = varying constants (depending on the material), called the "stress optic constants" for the particular material.

Light will propagate through the plate polarized in the principal planes, and the two orthogonal rays will accumulate a stress-induced, relative linear retardation,

$$\delta = hC(\sigma_1 - \sigma_2)$$

where h is the thickness of the plate, or more specifically the distance traveled by the light in the stressed plate. It is generally more convenient to express the relative retardation in radians. Thus the relative angular retardation, R, is

$$R = \frac{2\pi h}{\lambda} C(\sigma_1 - \sigma_2) \quad \text{.....} \quad 4.1$$

where R = angular shift between the two component vectors after passing through the stressed plate = $(2\pi/\lambda)\delta$

λ = wavelength of the monochromatic light traversing the plate

The above equation 4.1 expresses the stress optic law, which forms the foundation of photoelasticity. The stress-optic law states that the relative angular retardation, R, is linearly proportional to the difference in the in-plane principal stresses, $(\sigma_1 - \sigma_2)$, and to the thickness of the plate; R, the relative retardation, is inversely related to the wavelength of the light.

The stress optic law is more commonly written as

$$\sigma_1 - \sigma_2 = \frac{N f_\sigma}{h}$$

where $N = R/2\pi = \delta/\lambda$ = relative retardation in terms of complete cycles of the radiation used; N is also called the "fringe order" and is wavelength dependent

$F_\sigma = \lambda/C$ = material fringe value or fringe-stress coefficient with typical units of N/mm per fringe; It represents the principal stress difference necessary to produce unit change in the fringe order in a model of unit thickness.

4.5 PHOTOELASTIC MATERIALS

The properties desirable in a photoelastic material for a better analysis and results are as follows. A photoelastic model material has to be necessarily transparent if not crystal clear. For the production of an isochromatic pattern, which is the most common photoelastic operation, the stress-optical coefficient should be as high as possible. Further, in order that the shape of the model (when deformed under load) shall not differ appreciably from that of the prototype, the elastic modulus should be as high as possible. With respect to the mechanical properties, the usual requirements are high strength, linear proportionality between stress and strain, and freedom from creep. Since the results of photoelastic analysis are to be transferred to the prototype, linearity should exist between the stress levels and the order of fringes in photoelastic models. To conform to the basic assumption in mechanics of solids, the photoelastic material must be isotropic and homogeneous. This property is usually met, as the molecular chains of polymer are randomly oriented. The materials must have the required flowability in order that the castings of complicated shapes can be made. Most model materials exhibit initial stresses resulting from the manufacturing processes. These can be eliminated in some cases by annealing. To anneal a model, it is heated to a temperature above the softening point of the material and cooled at a very low rate to avoid freezing in thermal stresses. For the production of castings, the materials and casting procedure should be chosen to avoid the development of initial stresses during gelation and cure.

The epoxy resins and the polycarbonate resins are among the widely used photoelastic materials in the industry. The material that is being considered for the present analysis is SG95 provided by HEK GmbH, Germany. This resin is a specially formulated polyurethane resin that comes as a two-part mixture. Part 'A' is a based on a polymeric hydroxyl compound or polyol with catalytic additives, while part 'B' is invariably a di-isocyanate. The specifications of this resin and its properties were given in chapter 2. This resin is used with the rapid tooling equipment to cast the components under vacuum. These urethane resins have good optical and mechanical properties. These resins can be cast in vacuum allowing the fabrication of complicated parts amenable to photoelastic stress analysis. SG95 has a high modulus of elasticity as

compared to the other polyurethane resins. The properties of this resin as compared to other photoelastic resins are given in the Table-4.1.

	Epoxy	Polycarbonate	SG 95
Young's Modulus(MPa)	3,300	2,600	2,521
Matl. Stress Fringe Value	11 N/mm fringe	7 N/mm fringe	7.5 N/mm fringe
Poisson's ratio	0.37	0.28	-----

Table-4.1. Comparison of different Photoelastic resins.

4.6 PHOTOELASTIC TESTING METHODS

Photoelastic testing embraces three broad categories

- Two-dimensional model analysis
- Three-dimensional (stress-freezing) model analysis
- Photoelastic coating analysis

The focus of the present work is on two-dimensional and three dimensional analysis of rapid tooling components cast from the silicone molds using SG95 resin supplied by HEK GmbH, Germany. An attempt is made to calibrate the material and to look at the possibility of analysis of complex three-dimensional models using SG95 resin. With the standardization of this resin as a photoelastic material the stress analysis of any component can be done immediately by the fusion of Rapid Prototyping, Rapid Tooling and Digital Photoelastic Stress Techniques.

4.6.1 TWO DIMENSIONAL MODEL ANALYSIS

In two-dimensional analysis, the models cast from Silicone molds are analyzed. The models that are undertaken for the study are a circular disk under compression and a turbine blade. The finished model is then placed in a transmission polariscope, which

is usually equipped with loading frame, magnification device, and camera. Two-dimensional model analysis is normally employed during the early stages of design. Inexpensive plane-stress photoelastic models of part shapes, cross sections, and contours can quickly be made and tested to confirm the fine details of stress distribution and magnitudes, particularly at boundary edges and in tight fillets where maximum stresses are most likely to occur.

4.6.2 OUTLINE OF PHOTOELASTIC MODEL MAKING PROCEDURE

i. The CAD model of the part that is to be analyzed is prepared using PRO-Engineer modelling software. An STL file is created from this model and this is used an input to any Rapid Prototyping machine.

ii. The minimum slice thickness is taken to obtain a better surface finish and the model is manufactured in the RP machine (FDM / SGC).

iii. The model is polished to improve the surface finish. Once the model is prepared this is used as a master pattern to create a silicone mold in the MCP Vacuum casting machine. The procedure for making a silicone mold is explained in chapter 3 in detail.

iv. Components are cast in the Silicone mold using SG95 resin supplied by HEK GmbH, Germany. The procedure and the precautions to be taken for a better casting are explained in detail in chapter 3.

v. These components made out of SG95 are birefringent and can be easily analyzed using Digital Photoelastic techniques.

4.6.3 EXPERIMENTAL SET-UP FOR IMAGE CAPTURING

The full potential of photoelastic analysis can be achieved only if the image capturing is made simpler with the minimal hardware set-up. Fig.4.2 shows the loading frame used for conducting the tests. The figure is self-explanatory.

- **Loading arrangement for circular disc**

  The circular disc is loaded diametrically. To ensure a diametral load, the disc is mounted between two parallel flats, as shown in Fig.4.3.

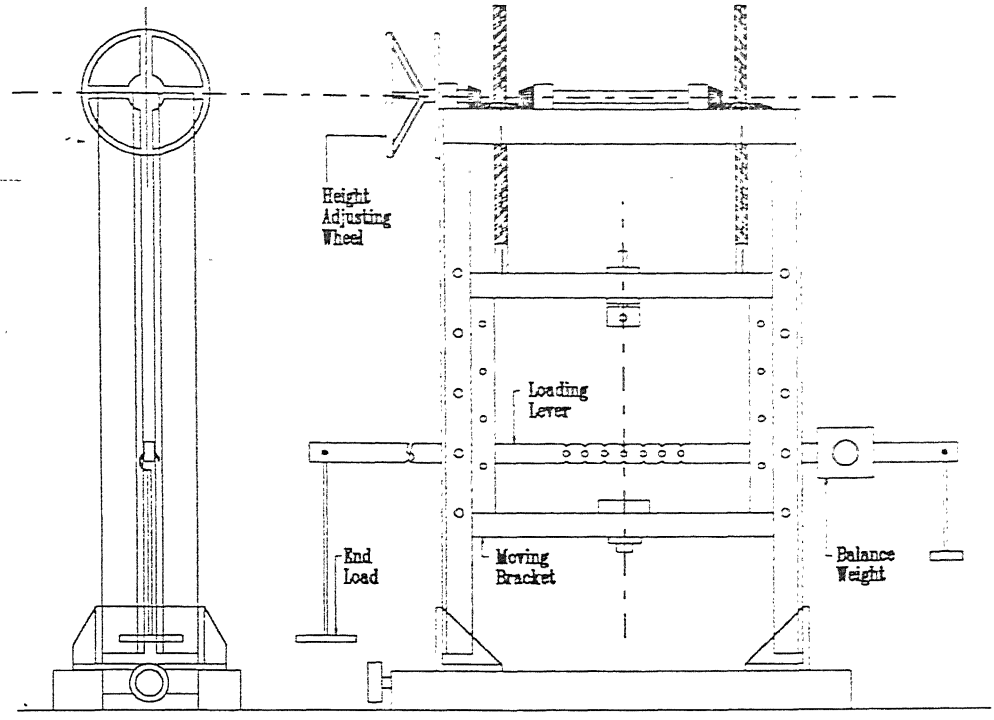

Fig.4.2: The loading frame

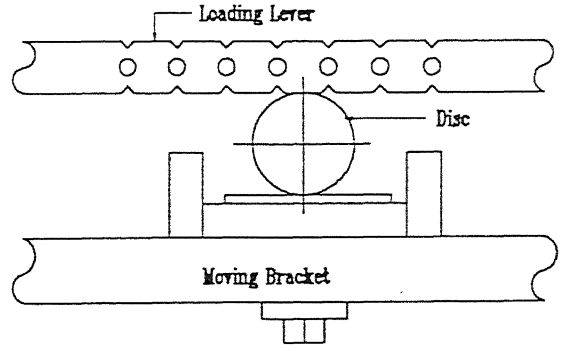

Fig.4.3: Circular disc under diametral load

- **Loading arrangement for a turbine blade**

  The turbine blade is loaded in tension and bending. For applying tensile load, the blade is mounted between two jaws of the standard universal machine. For bending load, a separate set-up on existing loading frame is prepared as shown in Fig.4.4.

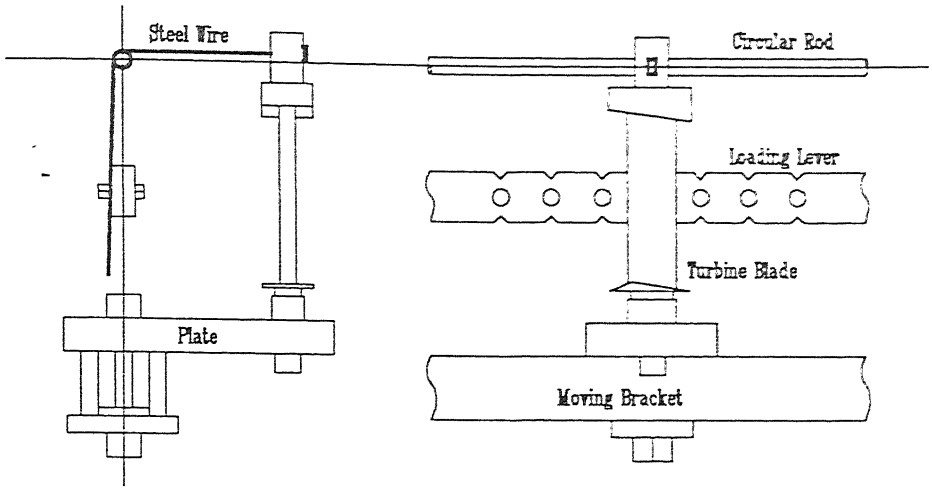

Fig.4.4: Turbine blade under bending load

- **Set up for Photoelastic analysis**

  A transmission polariscope is used for analyzing fringe patterns on the test parts.The main components of the transmission polariscope are the light source, a polarizer, two-quarter wave plates and an analyzer as shown in Fig. 4.1.

4.6.4 ANALYSIS OF FRINGE PATTERNS

The polariscope can be arranged in two different types;

1. Plane Polariscope: The polarizer and analyzer axes are crossed and the system produces dark field. The two contours namely Isochromatics and Isoclinics can be seen. An Isoclinic refers to the constant inclination and is the locus of points where the directions of the principal stresses coincides with a particular orientation of polarizer and analyzer combination. Isochromatic contour is the locus of points where the values of $(\sigma_1 - \sigma_2)$ are such as to cause a relative phase difference. Isochromatic represents the contours of constant color. Thus the principal stress direction and the principal stress difference $(\sigma_1 - \sigma_2)$ at any point can be viewed through the polariscope.

2. Circular Polariscope: In circular polariscope arrangement, along with the polarizer and analyzer plates, two quarter wave plates are provided. The system produces both dark and bright fields. The dark field set-up gives fringes representing an integer number of fringe orders i.e. 0,1,2 & so on. The bright field set-up gives fringes representing odd multiples of half integer i.e. 0.5,1.5,2.5 & so on. Thus using both the set-ups one can easily measure the fringe order at any point. Table-4.2 summarizes the arrangements for plane and circular polariscopes.

Determination of fringe order at a point:

White light gives colored fringes while monochromatic light gives black fringes. Colored fringe pattern is used to identify the integer fringe order using a color code (Table-4.3) in the dark field set-up. For quantitative measurement i.e., for fractional fringe orders, monochromatic light is used. For experimental purposes, the circular polariscope arrangement is used to measure the fringe order, which is sufficient for comparison of stress values in the model.

Set up	Polarizer and Analyzer	Quarter wave plates	Polariscope fields
Plane Polariscope	X	None	Dark
Circular Polariscope	X	X	Dark
	X	II	Bright
	II	X	Bright
	II	II	Dark
X : Crossed axes		II : Parallel axes	

Table-4.2 : Polariscope Set-ups

Colour	Approx. fringe order
Black	Zero
Gray White Yellow Orange Red	
Tint of passage (Purple)	One
Blue Green Yellow Orange Red	
Tint of passage (Purple)	Two
Green & so on	

Table-4.3. Colour code for Dark field

For measurement of fractional fringe order [10], **Tardy method of compensation** is used as explained below;

i. Determine the isoclinic at the point of interest.

ii. Rotate all optical elements forming a circular polariscope to this angle.

iii. The analyzer plate is rotated such that a fringe order passes through the point of interest.

iv. The fractional fringe order is **Integer fringe order** $\pm$ **(θ/180)°**,
where +ve sign is used when a lower order fringe coincides with the point of interest and -ve sign when a higher order fringe passes through the point of interest.

For more accurate results, an image of the fringe pattern is recorded using a CCD (Charged Coupled Device) [11] camera and then transferred to the PC.

Thereafter digital image-processing techniques for data reduction can be used for accurate analysis.

4.7 EXPERIMENTAL RESULTS

4.7.1 Models For Analysis

A circular disc under diametral compression and a turbine blade are the models selected to verify the new methodology for photoelastic analysis of rapid tooling models. This is because the models are easy to make, easy to load and a closer simulation to the theory is possible.

4.7.2 Circular disc under diametral compression

A circular disc with a diameter 60 mm and thickness 5.7 mm is made by RT process. The master pattern for the silicone mold (for a circular disk) was a circular disk made of epoxy material. The gates and risers are cut off and the surface is polished avoiding any scratches. Using Tardy Method of Compensation procedure the material stress fringe value is calculated to be 7.5 N/mm fringe.

$$F_\sigma = \textbf{7.5 N/mm per fringe}$$

4.7.3 Preliminary Analysis of Complex Shaped Objects

The turbine blade having twist is selected to study the analysis of complex shaped objects. Thus the objective is to see how far this approach is successful in revealing the stress picture. The dimensions are measured from an actual blade meant for MIG-21 gas turbine and using Pro-Engineer the CAD model is made. The RP model is obtained as discussed in Chapter 2. The slice thickness is taken to be 0.254 mm for the component made on the FDM machine from Stratasys Inc., and 0.15mm on the SGC machine from Cubital Inc., The surface finish of the SGC component was much better than the FDM component. Depending on the surface finish of the master pattern that is used for creating the Silicone mold, the transparency of the end component made by SG95 increases drastically. The better the surface finish of the

master pattern the greater is the transparency of the model. The component made from a silicone mold using an FDM component as a master pattern can be seen in the photographs shown below in Fig.4.5.

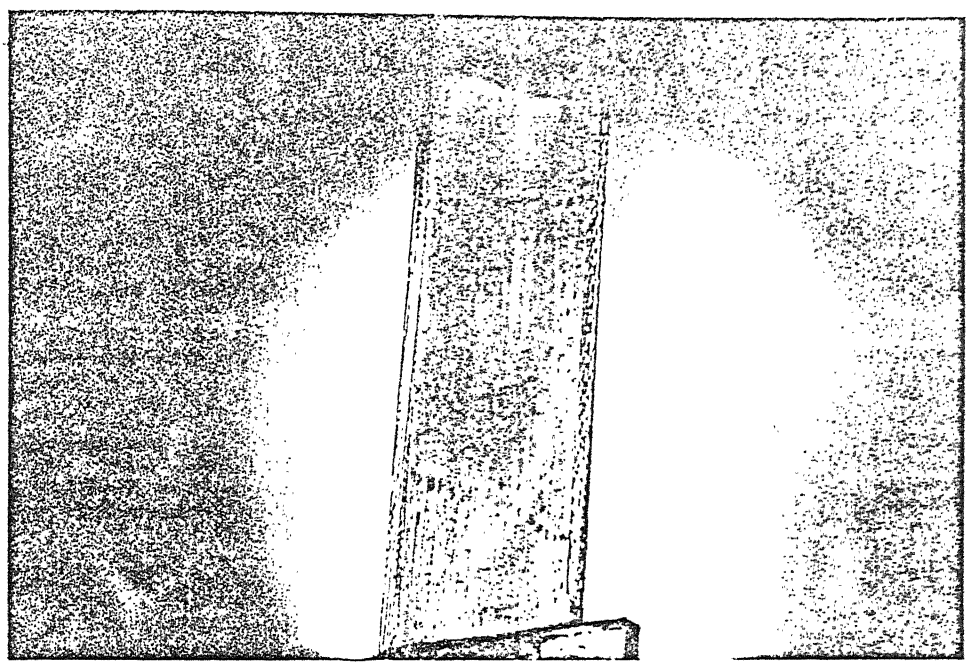

Fig.4.5. Fringe contours for turbine blade without any load (Master Pattern from FDM)

From the figure shown above, it can be clearly seen that there is a lot of residual stress locked in the model, cast from the Silicone Mold. The order of this stress is very high as is evident from the color coding shown in the Table-4.3. This high order stress is a bottleneck in the photoelastic analysis. They are very undesirable for the following reasons:

(1) Residual stresses are difficult to measure.

(2) They add to the stresses due to the applied load and hence hinder the analysis.

4.8 RESIDUAL STRESSES

The residual stresses are the major bottleneck in using the components made from the MCP - Vacuum Casting system for digital photoelastic stress analysis. Some causes for the residual stresses are listed below.

1) **Improper Mold design.** The runner and riser should be correctly placed so that the last sections to solidify (the thick sections) have enough material to allow for the shrinkage of the material. The runner is to be placed at the thicker sections.
2) Stresses arising due to the **shrinkage** of the material. Shrinkage stresses during polymerization are developed because of the thermal gradient set up by the exothermic reaction. The various kinds of shrinkage stresses that can cause residual stresses are explained in the Fig. 4.6.
3) Quick **change in sections** brings in a change in the solidification time of the thick and thin sections. This change in time will not allow for uniform shrinkage of the material that gives rise to residual stresses.
4) **Thermal Stresses** due to the temperature gradients.
5) **Inter-molecular stresses** arising due to the cross-linking between the molecules of different chains of the polymers.

In this work various ways for reducing the residual stress were tried out. Different ways that were chosen to solve the problem and the failure/success achieved thereof is discussed in the sections to follow.

4.8.1 CHANGE IN MOLD DESIGN

In the case of the turbine blade the runner and riser placement was as shown in Fig.4.7(a). As is evident from the figure the riser was placed on a section that was thin. This was thought of as introducing the residual stresses as the thick sections were not having enough material to support the shrinkage (as the thick sections are the last to solidify). To investigate this problem another mold was designed to analyze the change in the placement of the runner and riser on the residual stress of the end component.

The second time the riser was placed as shown in the Fig.4.7(b). The results were not encouraging, as there was no change in the residual stress of the end component as demonstrated in the color pictures.

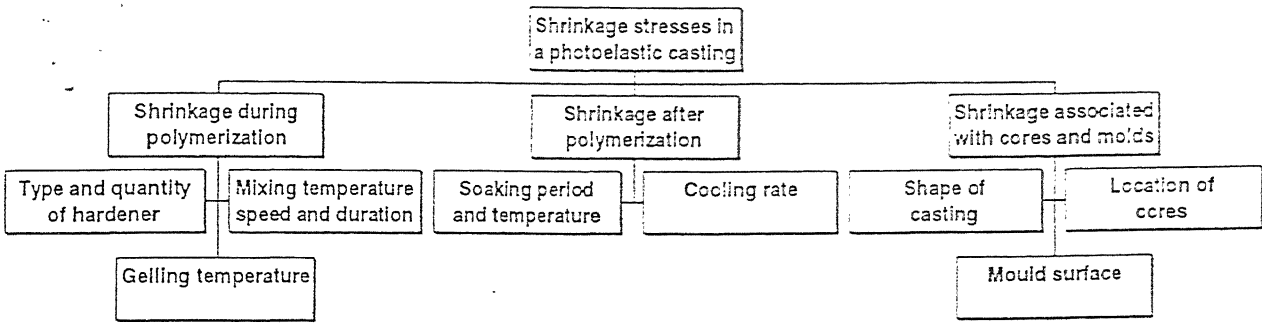

Fig.4.6. Shrinkage stresses in castings

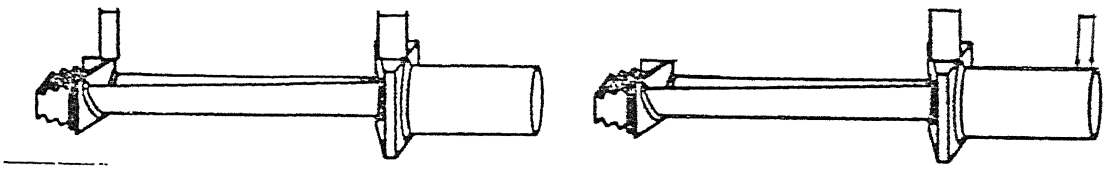

(a) (b)

Fig.4.7. Runner and Riser postioning in different molds.

4.8.2 STRESS ANNEALING

This is one of the common methods for relieving the stresses in the model. When the models are heated and taken to a temperature above the glass transition

temperature of the material the molecules are free to move and the stresses that are locked in are released. To remove the residual stresses the following procedure is to be followed: The model is placed on a flat surface if the model is a plate or in a liquid bath if the model has a complicated shape so that the model floats. The model with the supporting medium is placed in a stress freezing oven. The temperature is slowly increased to its critical temperature and the model is maintained at this temperature over a sufficiently long period of time depending upon the size of the model so that thermal equilibrium is reached. All the points in the model must have the same temperature for a certain period in the soaking cycle. At this stage the primary bonds break up and the loads on them are released. The cooling cycle is carried out at a very slow rate to avoid freezing of thermal stresses. This particular route was tried out for SG95 resin the heat deflection temperature of which is 70°C. The following different annealing cycles were followed to bring down the residual stress levels.

(a) The component was gradually heated from a temperature of 30° C to 55° C by increasing the temperature in increments of 5° C for every half an hour. The model was placed at 55° C for a period of four hours and then was allowed to cool in the furnace for a period of four to five hours.

(b) In the second attempt the same annealing cycle as used above was followed, but the temperature range was changed form 55°C to 60°C.

(c) In the third and fourth attempt the upper limit of temperature was changed to 65° C and 70° C.

In all the four cases the turbine blade was checked for any improvement in the residual stress. There was no improvement in the residual stress levels in all the cases.

4.8.3 VARIATION OF THE RATIO OF SG95A AND SG95B

The process of making the component in the silicone mold, as explained in chapter two, involves the mixing of the SG95A and SG95B resins in the ratio of 100:150. SG95 A contains different Poletherpolyols. The main component is a Polyoxypropylene - glycerolether. SG95 B contains 4,4'-Diphenylmethanediisocyanate as the monomer and prepolymers from MDI and Polyols. The Isocyanate groups OCN

of SG95 B react with the alcoholgroups OH of the Polyol of SG95 A. Hence the end product contains long chains of Polyol-Isocyanate groups and in addition cross connections between these chains. Another school of thought has been that these cross-connections and chemical bonds between different chains were the root cause of the residual stress. Experiments were conducted to observe the effect of the variation of the amount of SG95 A on the residual stress. The actual ratio in which the amount of SG95 A and SG95 B are mixed is 2:3. Experiments have been conducted by varying this ratio to 1.75:3 and 1.6:3. All the other parameters like the mixing time, curing time and the curing temperature were maintained constant during the experimentation. A significant breakthrough has been achieved in reducing the residual stresses by varying this ratio. The photographs of the turbine blade, without any load, for different ratios of the resin in mercury vapor lamp are shown in Fig.4.8. The photographs for turbine blade (Fig. 4.8 (iii) & (iv)) with a bending load of 30.76 N under sodium vapor lamp are juxtaposed for comparison.

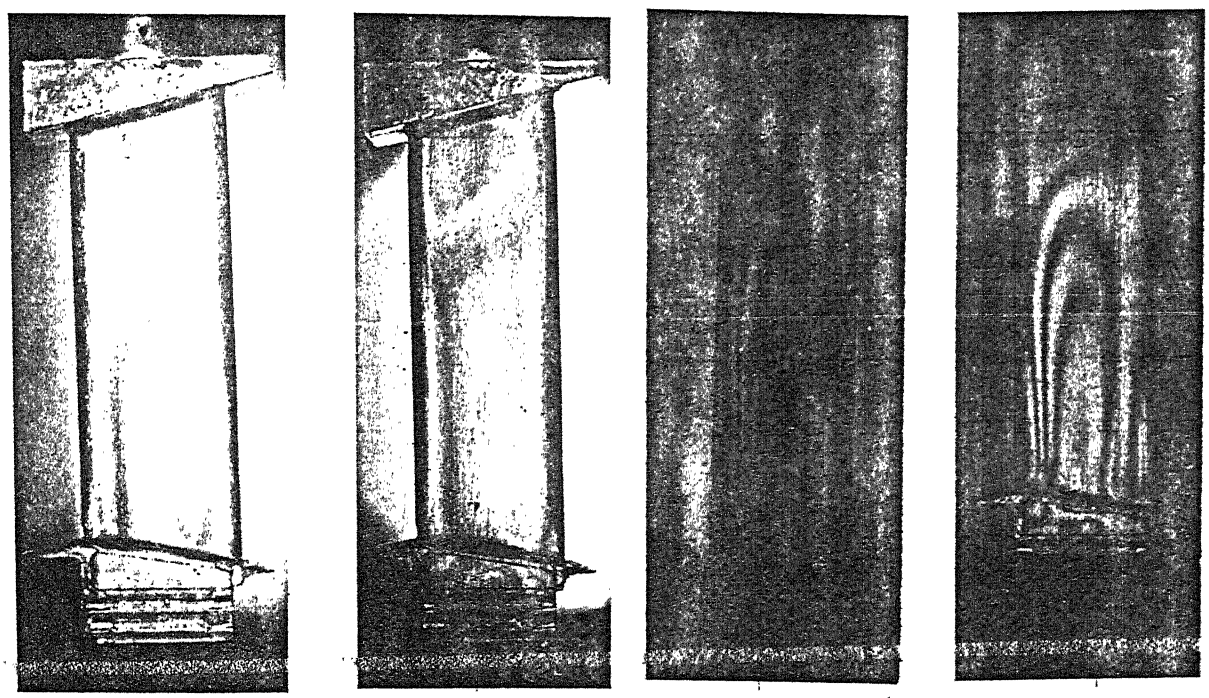

(i) **(ii)** **(iii)** **(iv)**

Fig.4.8(a) Ratio = 2:3 (i) & (iii) Dark field (ii) & (iv) Bright field

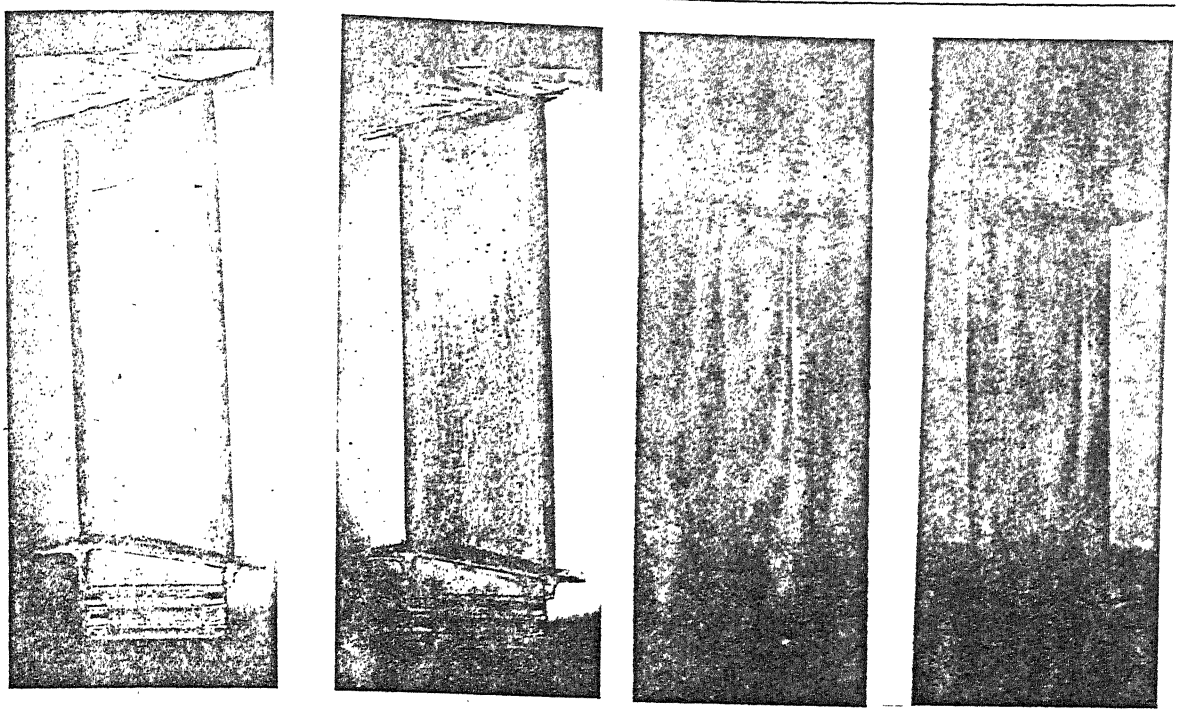

(i) (ii) (iii) (iv)

Fig.4.8(b) Ratio = 1.75:3 (i) & (iii) Dark field (ii) & (iv) Bright field

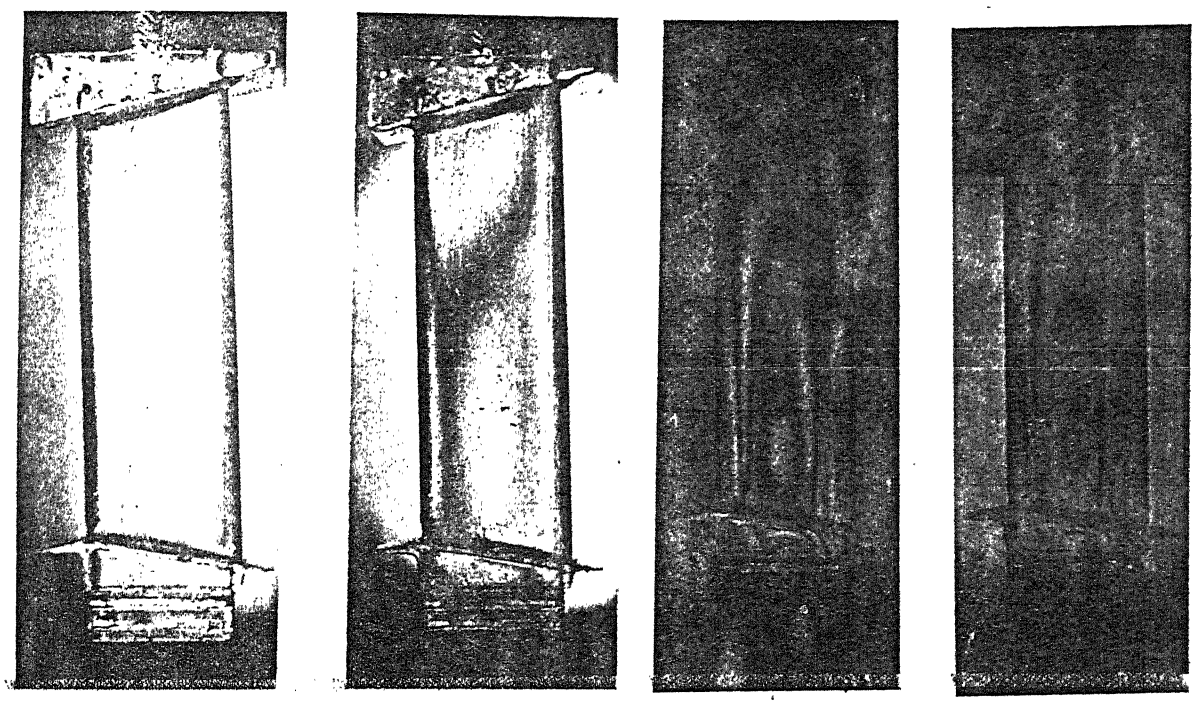

(i) (ii) (iii) (iv)

Fig.4.8(c) Ratio = 1.6:3 (i) & (iii) Dark field (ii) & (iv) Bright field

Fig.4.8. Comparison of Residual stresses for different ratios of SG95

4.8.4 STANDARDIZATION OF THE MATERIAL

With the variation in the ratio of the resin components the material structure of the component changes and this material has to be calibrated again. Circular disks of these ratios were cast from the silicone molds and experiments were again conducted to obtain the material stress fringe value. DIP procedures were used to calculate the F_σ value for these turbine blades. The circular disk made with the ratio of 1.6:3 of A:B was analysed by applying a load of 447.6 N and that with 1.75:3 is analysed by applying a load of 732.6 N. The fringe contours for these models are as shown in the Fig. 4.9(a) and Fig. 4.9(b). The reconstructed fringe pattern with the data points echoed back for the different ratios of the resin are shown in the Fig.4.10(a) and Fig.4.10(b).

F_σ for circular disk with A:B ratio as 1.6:3 is = 4.8 N/mm per fringe

F_σ for circular disk with A:B ratio as 1.75:3 is = 6.5 N/mm per fringe

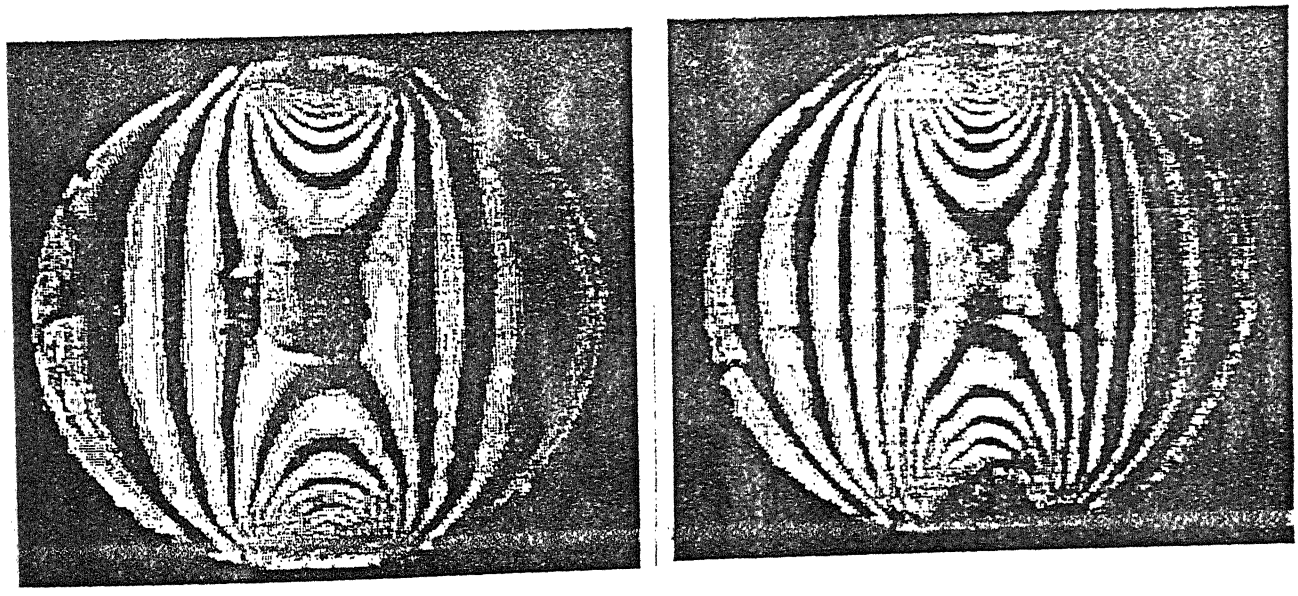

(a) Load of 447.6 N
[Ratio = 1.6:3]

(b) Load of 732.6 N
[Ratio = 1.75:3]

Fig. 4.9 Fringe contours for a circular disk

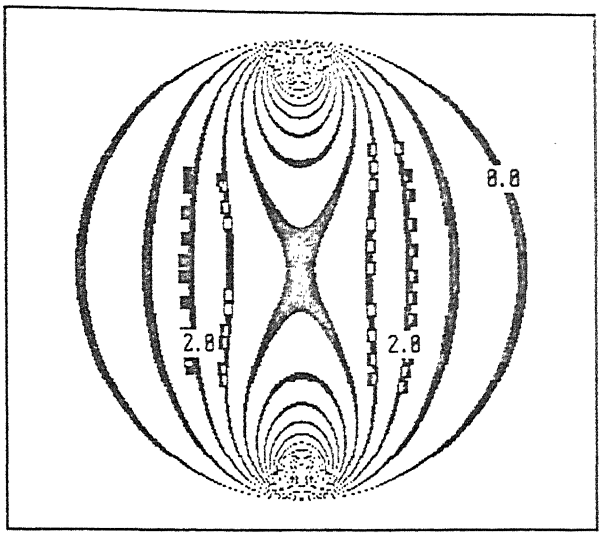

Fig.4.10(a) [Ratio of SG95 A:B = 1.6:3]

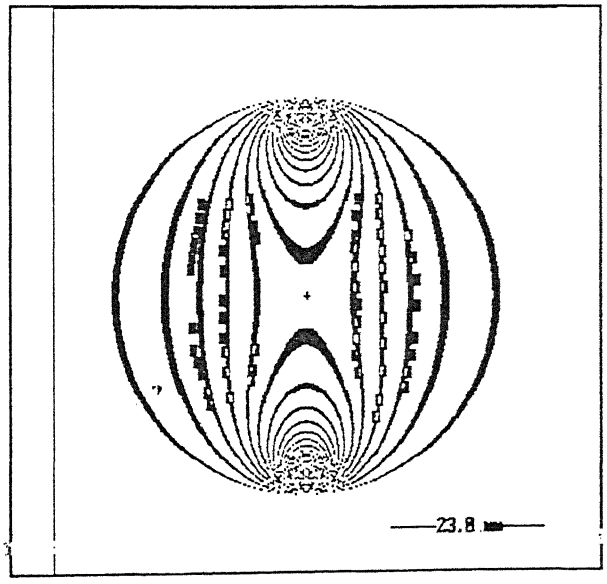

Fig.4.10(b) Ratio of SG95 A:B = 1.75:3

Fig. 4.10 Reconstructed fringe pattern with data points echoed back

4.9 THREE DIMENSIONAL MODELS - STRESS FREEZING

As the design nears completion, a more comprehensive photoelastic stress-freezing analysis may be desirable. The model is loaded and subjected to a stress-freezing process, after which it is sectioned to permit removal of slices through various planes of interest. Slice examination in a transmission polariscope reveals the complete stress distribution in the plane of the slice.

Historically, photoelastic models for the three-dimensional analysis have been made by machining from solid blocks or rounds, cast to shape, or fabricated by cementing flat and formed sheets together. The model materials are specially blended epoxy resins that have the desired physical and optical properties for photoelastic analysis. But with the advent of the Rapid Prototyping and Rapid Tooling technologies the three dimensional models can be easily made. The concept of stress freezing and the feasibility of the present models, made by MCP Vacuum Casting process, to stress freezing is discussed herewith.

4.9.1 THE PRINCIPLE BEHIND STRESS FREEZING

The phenomenon of stress freezing can be attributed to the diphasic behavior of certain polymeric solids. The molecules of these materials are held together by two distinct sets of bonds. When such a material is subjected to a load at room temperature, both sets of bonds are in effect. But if the temperature is gradually increased to a specific critical level [typically 140 - 275 deg F (60 - 135 deg C) depending on the type of material, one set of bonds relaxes and the other set carries the whole load. The modulus of elasticity drops rapidly, and relatively large elastic deformations occur.

When the temperature of the model is lowered from the critical temperature toward room temperature with the loads still applied, the secondary bonds reform and lock in the molecular deformations. The soft material becomes rigid again. As a result, if the model is cooled and the loads are not removed until room temperature is restored, no external loads are needed to maintain the deformation in the network of primary elastic bonds. The hardened secondary bonds permanently maintain the

deformations with virtually no change in magnitude. The stresses are "frozen" in place. As long as the temperature is kept below the critical point, the stresses will remain permanently.

Since the freezing process occurs at a molecular level, thin slices may be cut from the solid model for examination without disturbing the deformation or the model's photoelastic properties. Once the slices have been removed from the model, they are examined in a transmission polariscope for analysis. More recently, new resin materials used to manufacture rapid tooling models by using patterns from FDM and SGC processes have been developed, which make them suitable for photoelastic analysis. Thus, these models, in addition to their other primary uses in the design cycle, can also be used to validate and refine finite-element analysis by subjecting them to the stress-freezing process.

4.9.2 EXPERIMENTAL PROCEDURE

A circular disk made from the silicone mold using SG95 resin was considered for experimentation to look at the feasibility for stress freezing. Loading of the model is prescribed according to the sketch shown in Fig 4.11. The circular disk was loaded with a weight of 10kg as shown in the figure. A test fixture as shown in Fig. 4.11 was used to support the model in the stress-freezing oven. The model was then heated to its stress-freezing temperature of 150 deg F (65 deg C), gradually over a period of time. The temperature of the oven is gradually increased from 35°C to 65°C in steps of 5°C per half an hour.

Then a resultant dead-weight load of 10 Kgf was applied to the circular disk which was sufficient to produce enough deformation to create a strong photoelastic signal. The loaded model was then allowed to soak at the stress-freezing temperature for approximately two hours, after which it was slowly furnace cooled to room temperature. (The rate of cooling depends on the volume of the model.)

For thin sections, cooling can be accelerated, while thicker sections may require a cooling cycle as low as 1°C per hr. Choosing the proper cooling cycle is important to ensure thermal uniformity throughout the volume of the model to eliminate unwanted

thermal stresses from developing during the stress-freezing process. For the circular disk model, the rate of cooling was 1°C /hr.

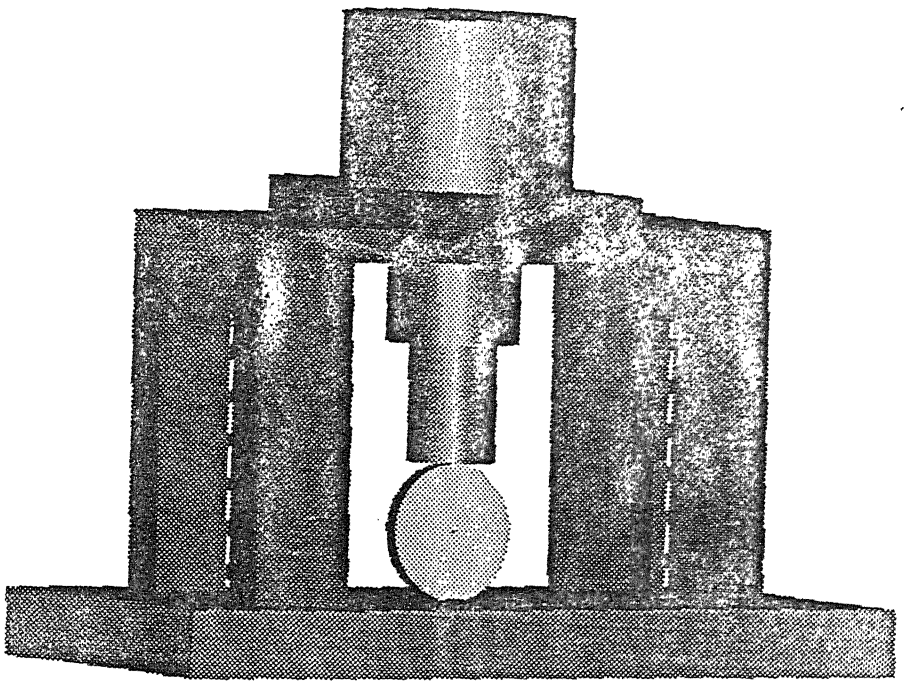

Fig.4.11. Loading frame for stress freezing of the circular disk.

After stress-freezing, the loads were removed from the model and it was ready for slicing. Stresses can be directly determined only on principal slices, planes about which the shape of the part and positioning of the load are symmetrical. Since principal stresses are known to be parallel and perpendicular to the principal plane, photoelastic readings perpendicular to these stresses provide a direct evaluation of stress magnitude. For slices removed from a non-principal plane, additional measurements and sub-slicing is necessary to yield the values of the individual principal stresses. For the circular disk two holes and a slot were cut to observe if there is any distortion in the stress field due to machining operations. The holes were drilled using a drilling

machine using a lot of coolant whereas a slot was cut in the model by a milling cutter. The stress frozen circular disk was placed in the polariscope and the stress field was observed for any distortions. There were no distortions observed in the stress field of the circular disk. Figures 4.12(a) and 4.12(b) show the dark and bright field isochromatics of the stress frozen disk. The respective dark and bright field images after cutting the slot and the holes are shown in Figures 4.12(c) and 4.12(d). Using a DIP procedure, the material stress fringe value is calculated and found to be 1.03 N/mm per fringe. Fig.4.13 shows the reconstructed fringe pattern with the data points echoed back showing self-consistency in the analysis. The whole experiment testifies that the resin SG95 is amenable to stress freezing and complex three-dimensional models can be easily analyzed using the present route of analysis described in this work.

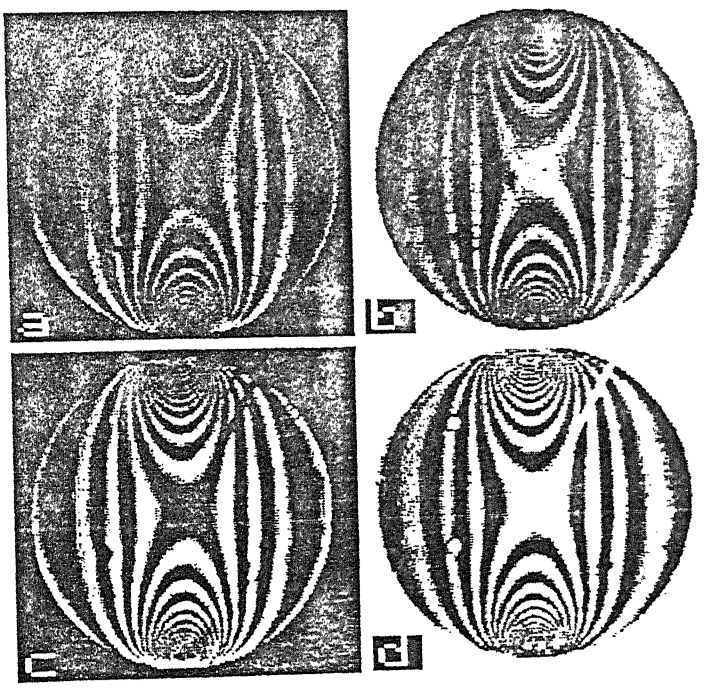

Fig. 4.12. Demonstration of stress freezing capability of the resin used: Stress frozen circular disk (a) Dark field (b) Bright field (c) & (d) same as (a) & (b) but after the introduction of two holes and a slot.

To reduce the stresses in the model, variation of the ratios of the resin were tried out. An investigation of the stress freezing ability of these models has also been tried out. The circular disks of diameter 60 mm with ratios of SG95 A to SG95 B as

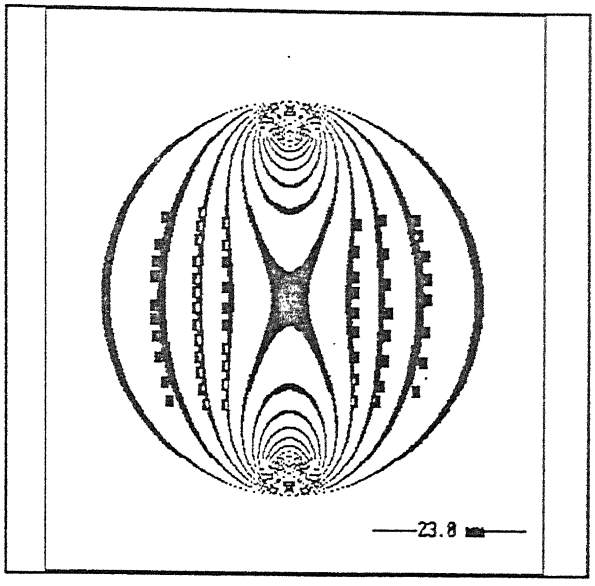

Fig. 4.13. Reconstructed fringe pattern with data points echoed back. [Ratio 2:3]

1.6:3 and 1.75:3 were manufactured. They were stress frozen in an oven under a dead weight load of 78.48 N. The temperature cycle through which these models were taken was the same as explained above for the circular disk. The fringe patterns are as shown in the Fig. 4.14 (a) and Fig. 4.14 (b). The reconstructed fringe pattern with the data points echoed back [Ratio = 1.75:3] is shown in Fig. 4.15. The F_σ value for the circular disk with ratio of 1.75:3 is 1.61. As seen from the figure the contours for the disk made with the ratio 1.6:3 are not good and hence the analysis was not possible. The stress freezing capability for this ratio of the resin has to be investigated further on. It could be tried out using higher loads while stress freezing it.

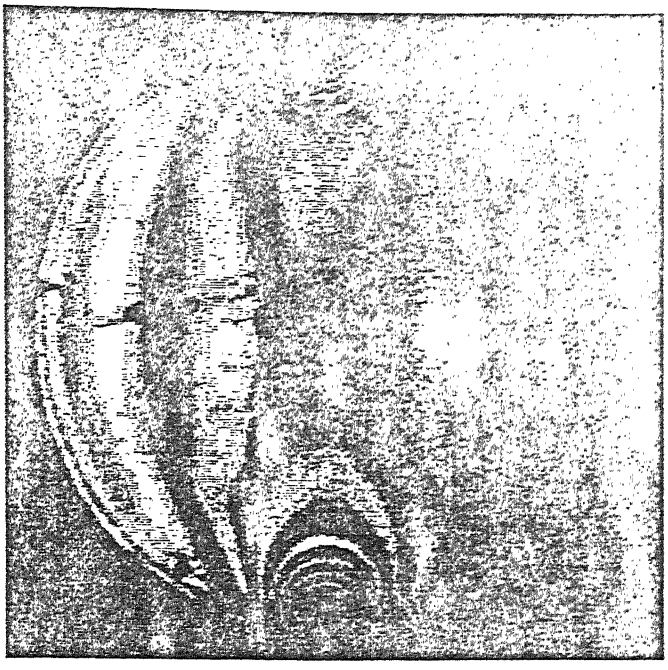

Fig. 4.14 (a) Fringe patterns for a stress frozen circular disk [Ratio = 1.75:3]

Fig. 4.14 (b) Fringe patterns for a stress frozen circular disk [Ratio = 1.6:3]

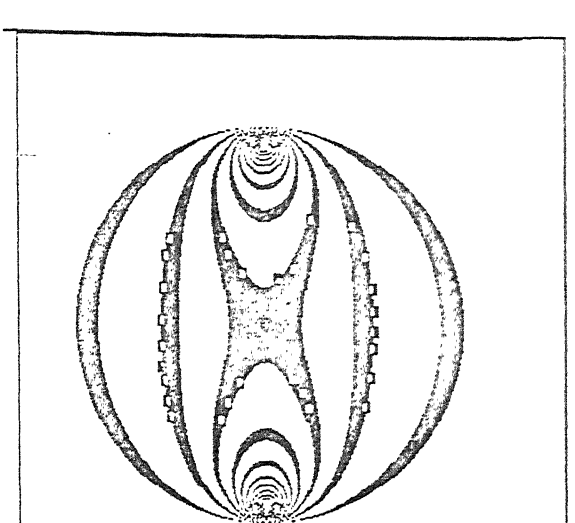

Fig. 4.15 Reconstructed fringe pattern with data points echoed back for stress frozen circular disk [Ratio = 1.75:3]

A comparative study of the ratios of the resins for SG95 is given in the Table-4.4 below.

F_σ	SG95 2:3	SG95 1.75:3	SG95 1.6:3
Material stress fringe value at room temp.	7.5	6.5	4.8
Material stress fringe value at stress freezing temp.	1.03	1.61	------

Units of material stress fringe value are N/mm per fringe

Table-4.4 Comparative study of F_σ for the resin SG95

For stress-freezing tests on other rapid tooling components, the analysis time will depend on a number of factors:

(a) The design complexity of the part for which a loading fixture must be fabricated;

(b) The stress freezing temperature cycle (which is dependent upon the bulk of the model);

(c) The number of slices to be extracted for analysis.

However, the whole process is by far much faster than could be achieved in the past because of the quick availability of the model from Rapid Tooling. There are some differences in the physical and optical properties of the resin SG95 used to make the photoelasticity models when compared to conventional photoelastic epoxies used for stress-freezing. The most noticeable difference is the optic response at stress-freezing temperature for the two materials. In conclusion, photoelastic analysis of Rapid Tooling models using SG95 resin shows that the stress-freezing method is fast and informative. It is an excellent way to validate stress information obtained by numerical methods such as FEA, especially in areas of "tight fillets" or complex geometry.

Chapter 5

FINITE ELEMENT ANALYSIS

5.1 FINITE ELEMENT MODELLING AND ANALYSIS

Finite Element Method is a powerful numerical technique for approximate solution of continuum mechanics. It is an approximate method, since a continuum with infinite number of degrees of freedom is replaced with a discrete system with finite number of degrees of freedom. The method involves subdividing a continuum into a finite number of regions called elements connected at finite number of points called nodes. An approximate admissible solution is constructed over the assemblage of elements, and the solution continuity is maintained at the inter-element boundary.

5.2 LINEAR STATIC ANALYSIS

In linear static analysis loads may consist of concentrated nodal forces, non zero specified displacement, thermal loading and body forces due to gravity, angular velocity and angular acceleration.

The total potential of an elastic body under general loading may be defined by

$$\Pi = U + V \tag{5.1}$$

where

U is the strain energy of the body and

V is the potential energy of the applied load

The principal of minimum potential energy states that among all the admissible displacement fields u which satisfies the prescribed kinematic conditions, the actual displacement is the one that makes the total potential energy stationary. Therefore Eq. 5.1 gives

$$\delta \Pi = \delta U + \delta V \tag{5.2}$$

where

$$\delta U = \int_v \sigma^t \delta \varepsilon dV \tag{5.3}$$

$$-\delta V = \int_v \delta u^T b dV + \int_A \delta u^T t dA + (\delta \bar{u}^c)^T p_c \tag{5.4}$$

where

u and c list the components of the stress and strain tensor in a vector form

b is the body force and

t is surface traction vector

u is displacement vector

$\bar{u}^c$ is a vector listing the displacement components corresponding to the concentrated forces

Mathematically,

$$\sigma^t = [\sigma_{xx}, \sigma_{yy}, \sigma_{zz}, \sigma_{xy}, \sigma_{yz}, \sigma_{zx}] \tag{5.5}$$

$$\begin{aligned} \varepsilon^t &= [\varepsilon_{xx}, \varepsilon_{yy}, \varepsilon_{zz}, 2\varepsilon_{xy}, 2\varepsilon_{yz}, 2\varepsilon_{zx}] \\ &= [\varepsilon_{xx}, \varepsilon_{yy}, \varepsilon_{zz}, \gamma_{xy}, \gamma_{yz}, \gamma_{zx}] \end{aligned} \tag{5.6}$$

$$b^T = [b_x, b_y, b_z] \tag{5.7}$$

$$t^T = [t_x, t_y, t_z] \tag{5.8}$$

$$u^T(x, y, z) = [u_x, u_y, u_z] = [u_1, u_2, u_3] \tag{5.9}$$

Equations 5.2 through 5.4 indicates that for an arbitrary virtual displacement δu satisfying the prescribed kinematic boundary conditions, the virtual work done by the internal forces is equal to the virtual work done by the external forces. This is exactly the principal work. It is important to note that the principal of virtual work holds for any kinematically admissible virtual displacements and it is independent of

the material stress strain relationship. In finite element analysis, a continuum is discretized by a number of suitable finite elements, which are interconnected through nodal points on the boundaries of the elements. The total potential of the continuum Π, may be considered as the sum of the individual element contributions Π^e so that

$$\Pi = \sum_{e=1}^{m} \Pi^e \tag{5.10}$$

where

m is the number of elements.

5.3 PRO-FEM TO NISA

Among the models studied, the turbine blade is a complicated 3D blade. An attempt has been made to evaluate the stress field by FEM. As geometric modeling for complex shapes in NISA is very difficult, the FEM modeling is done using Pro-FEM on existing model and the problem is solved and post-processed in NISA. The procedure followed for the analysis is given below;

i. The geometric model prepared in Pro-Engineer is taken as basic model.

ii. The material and its properties are defined.

iii. The boundary conditions are specified.

iv. The mesh of tetrahedral elements with default element size is created having 13448 nodes and 7566 elements (Fig.5.1).

v. The FEM file is stored with .fnf extension.

vi. The .fnf file is imported in NISA which contains the information about material properties, nodes, elements and boundary conditions.

vii. The database (.dbs) file and NISA (.nis) file are stored.

viii. The static analysis is carried out on NISA file, which gives the output file for postprocessing.

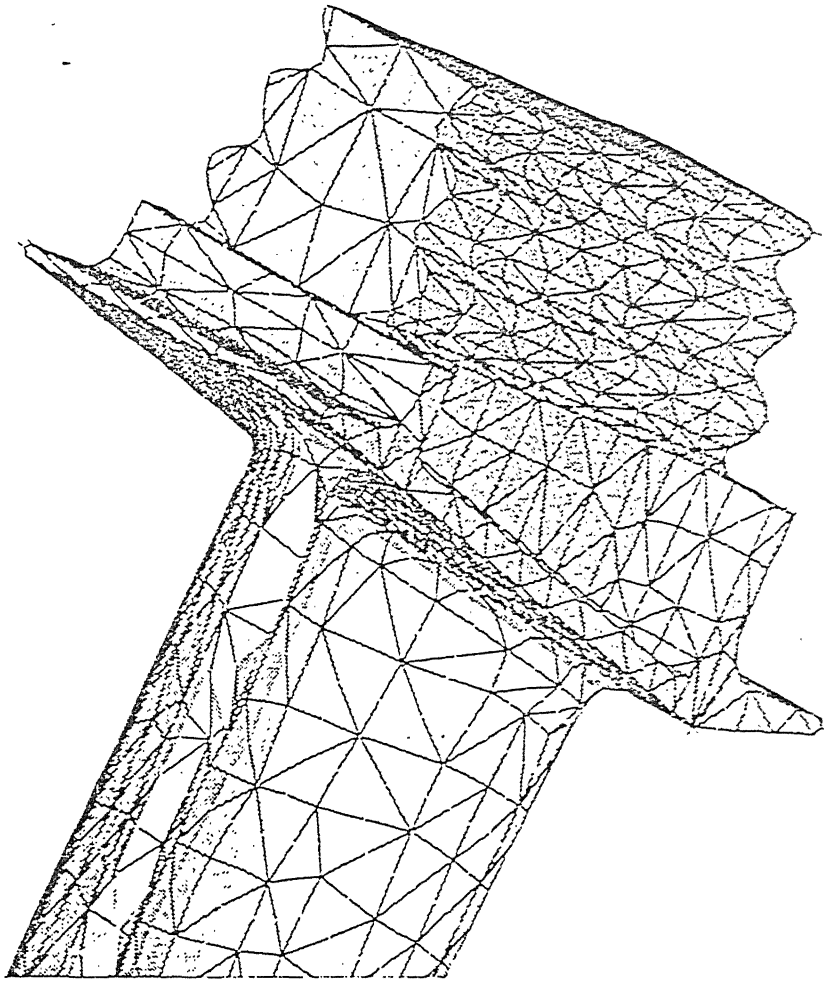

Fig. 5.1 Mesh of Tetrahedral elements

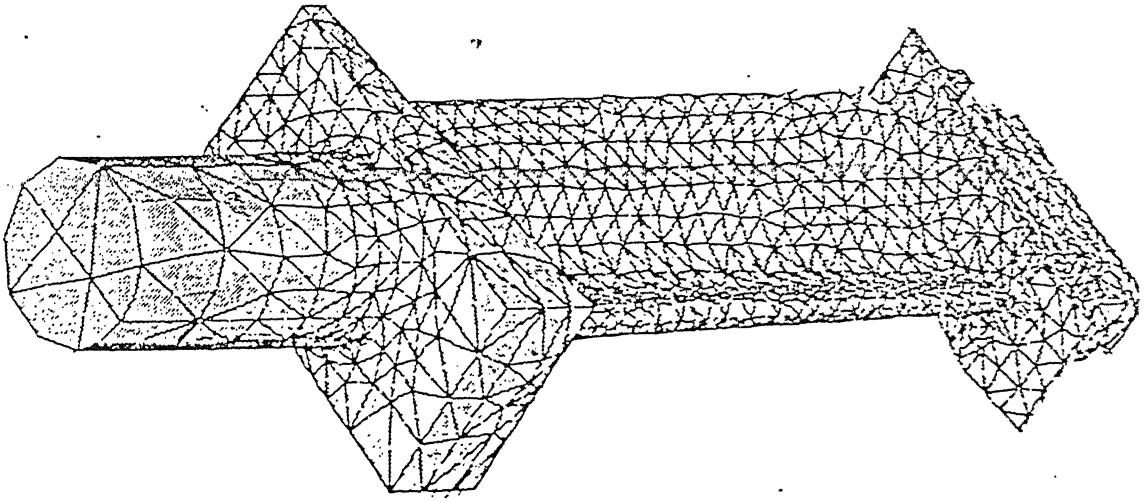

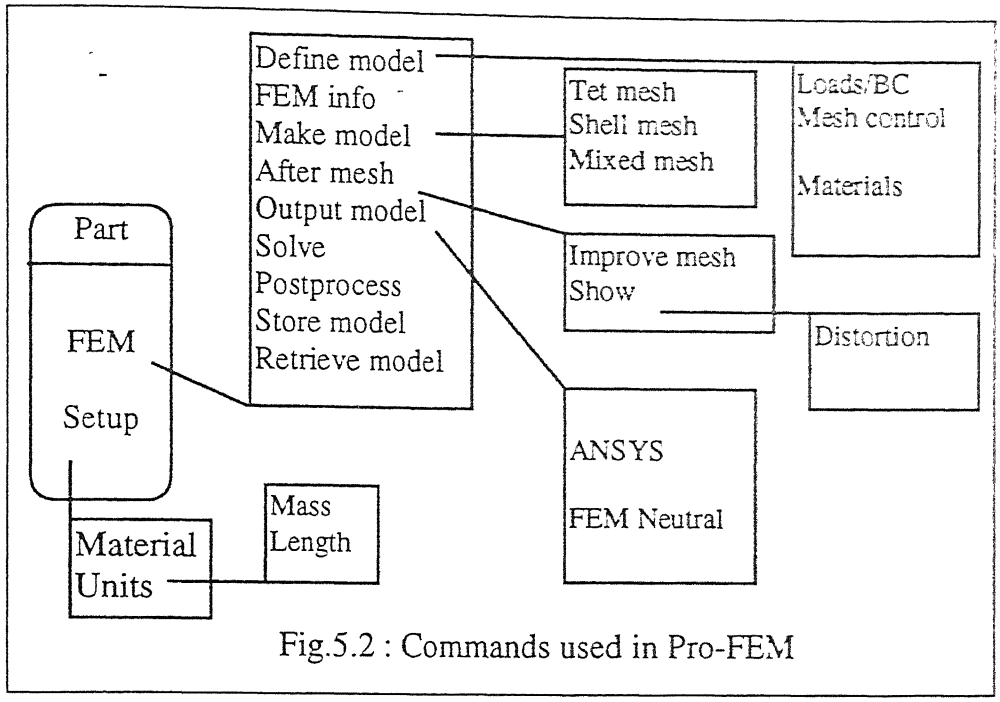

Fig.5.2 : Commands used in Pro-FEM

5.4 NISA SOFTWARE PROGRAM

NISA (Numerically integrated elements for System Analysis) is a general purpose program to analyse a wide spectrum of problems encountered in engineering mechanics. NISA has beeen used for carrying out the the Finite Element Analysis in the present study.

5.4.1 ELEMENT TYPE:

A 3-D 10-noded solid tetrahedron element is used in the present analysis. A typical ten noded element is shown in the Fig. 5.3.

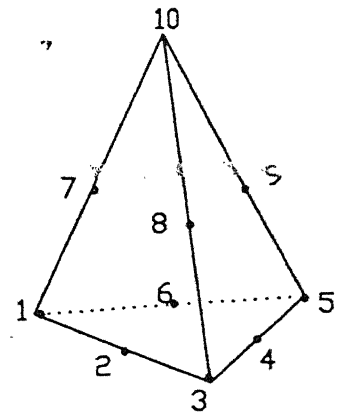

Fig. 5.3 3D Solid, 10 Noded Tetrahedron element

The 3-D element used is based on a general state of stress characterized by six components $(\sigma_{xx},\sigma_{yy},\sigma_{zz},\tau_{xy},\tau_{yz},\tau_{zx})$. The element has three translational degrees of freedom per node (u_x,u_y,u_z) and are suitable for modelling 3D solid structures with general loadings. These elements are isoparametric with the following shape function relations for both displacement and coordinates:

$$u=\sum_{i=1}^{n}N_i(\xi,\eta,\varsigma)\bar{u}_i \qquad x=\sum_{i=1}^{n}N_i(\xi,\eta,\varsigma)\bar{x}_i$$

$$v=\sum_{i=1}^{n}N_i(\xi,\eta,\varsigma)\bar{v}_i \qquad y=\sum_{i=1}^{n}N_i(\xi,\eta,\varsigma)\bar{y}_i$$

$$w=\sum_{i=1}^{n}N_i(\xi,\eta,\varsigma)\bar{w}_i \qquad z=\sum_{i=1}^{n}N_i(\xi,\eta,\varsigma)\bar{z}_i$$

where $\bar{u}_i,\bar{v}_i,\bar{w}_i$ are the nodal point displacements in x,y and z directions respectively.

$\bar{x}_i,\bar{y}_i,\bar{z}_i$ are the nodal point coordinates and

$N_i(\xi,\eta,\varsigma)$ are the element shape functions

For a 10-noded element;

$L_1 = 1-\xi-\eta-\zeta$ $\qquad$ $L_2=\xi$

$L_3=\eta$ $\qquad$ $L_4=\zeta$

$N_1 = L_1(2L_1 - 1)$ $\qquad$ $N_2 = 4L_1L_2$

$N_3 = L_2(2L_2 - 1)$ $\qquad$ $N_4 = 4L_2L_3$

$N_5 = L_3(2L_3 - 1)$ $\qquad$ $N_6 = 4L_3L_1$

$N_7 = 4L_1L_4$ $\qquad$ $N_8 = 4L_2L_4$

$N_9 = 4L_3L_4$ $\qquad$ $N_{10} = L_4(2L_4 - 1)$

The 3D solid elements represents a 3-D state of stress. Hence they are suitable for modelling 3-D solid structures with general loadings. In the under consideration at any point in the body the stresses are three dimensional and more over the information to model it as two dimensional is less to make sufficient and suitable assumptions to do so. In the present problem there is a bending load and hence the need for a 3-d analysis

5.5 TURBINE BLADE MODELING AND ANALYSIS

The turbine blade is loaded using a loading fixture as shown in Fig. 4.4. in chapter 4. The bending load is applied as shown in the same figure. The load that is applied on the turbine blade is through a hole made in the cylindrical portion of the blade. A wire with a stopper at one end is inserted through the hole and the other end of this wire is fixed to the loading bar of the equipment. The load applied at the end of the loading bar is magnified approximately 4.48 times. This load is modeled as a load applied on a node on the cylindrical surface, the direction of which is normal to the cylindrical surface. The load that is applied on the turbine blade is 0.7Kgf. The actual magnitude of the load applied on the node would be equal to 30.46 N. The difference in the first principal stress and second principal stresses were also computed using NISA. The procedure to be followed in this computation is indicated in the Fig. 5.4 shown below.

5.5.1 BOUNDARY CONDITIONS

With reference to the figure shown in chapter 4 the lower corrugated part of the turbine blade is fixed in a chuck in the loading fixture. This part of the turbine blade will not have any translations or rotations. Hence all the x,y,z translations are made zero on the lower plane.

5.5.2 RESULTS

In this section, the results of the present analysis are presented.

A) **Mesh Details:**

Due to the complexity of the model the mesh has been generated in the Pro-FEM package.

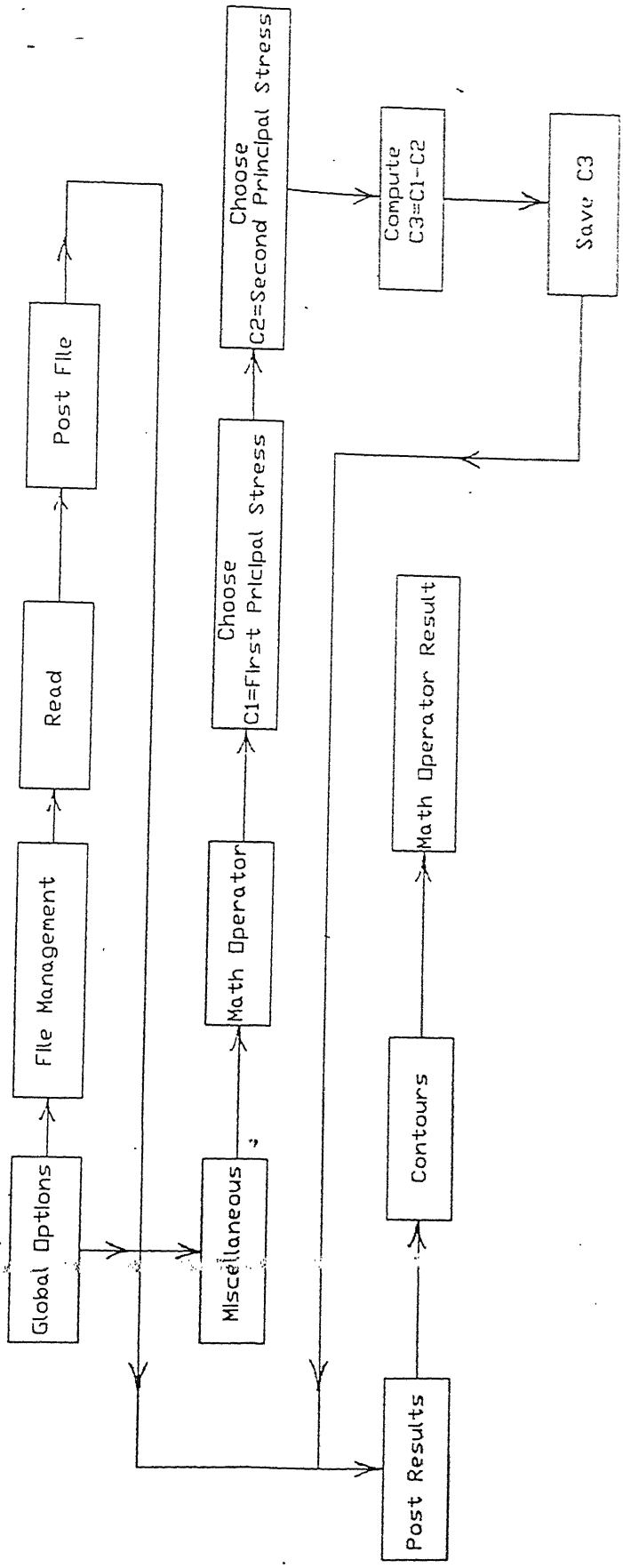

Fig. 5.4 NISA Commands for plotting the difference of first and second principal stress contours

10-noded 3-D solid tetrahedron element.

Discretization:

Total number of elements =7566

Total number of nodes =13448

Number of degrees of freedom/node = 3

B) **Material Properties :**

The material of the specimen is SG95 (isotropic material)

Young's Modulus, E =2521 MPa

Poison's Ratio, υ =0.33

5.5.3 EXPERIMENT NO. 1.

Force boundary Conditions:

A point load of 30.76N is applied horizontally on the node no. 1932, to simulate a bending load. The various contour plots are as shown in the Fig. 5.5.

5.5.4 EXPERIMENT NO 2:

Force boundary Conditions:

Uniform pressure of 2 MPa is specified at the top face to simulate tensile load. The contours are as shown in the Fig.5.6.

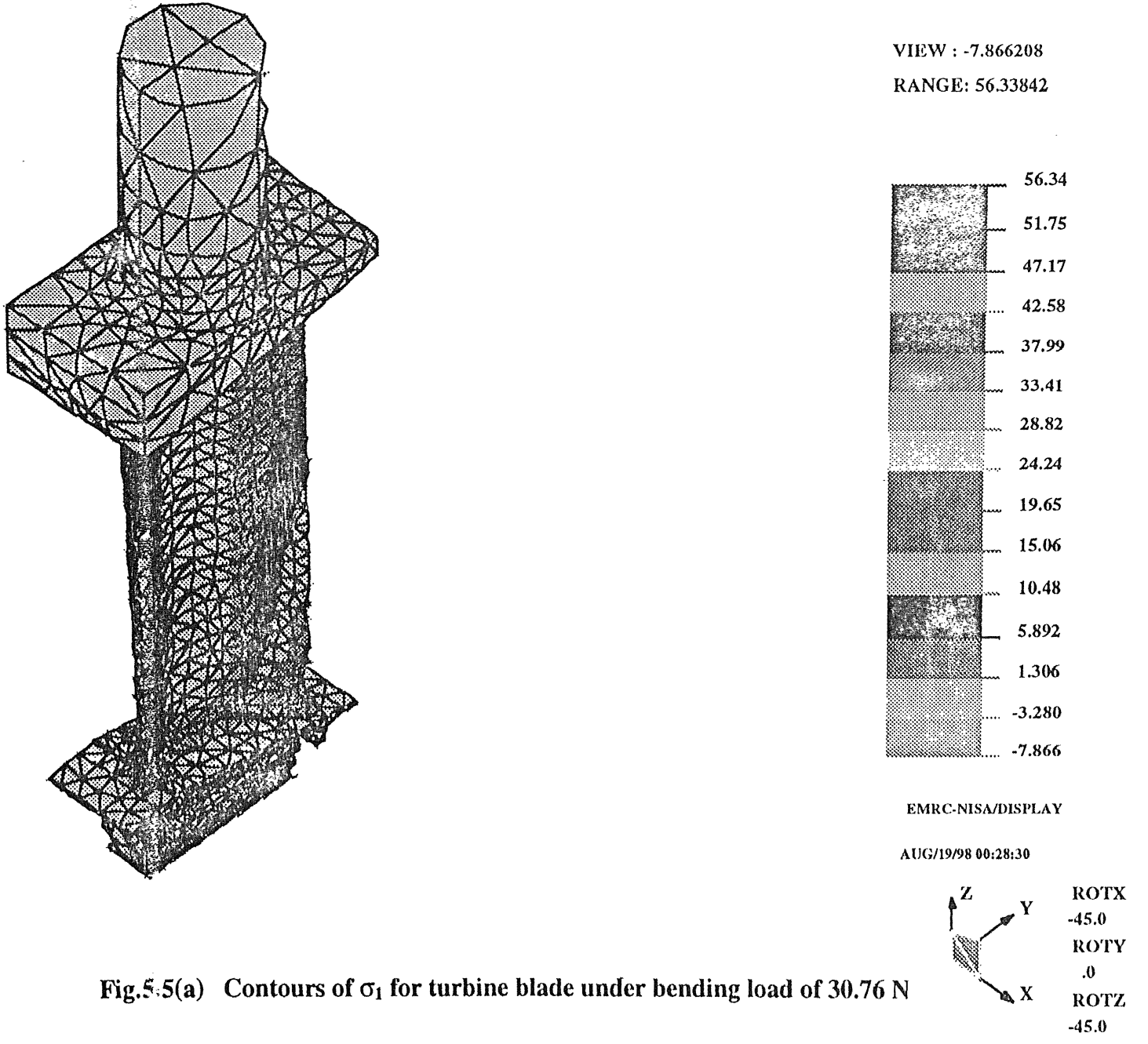

Fig.5.5(a) Contours of σ_1 for turbine blade under bending load of 30.76 N

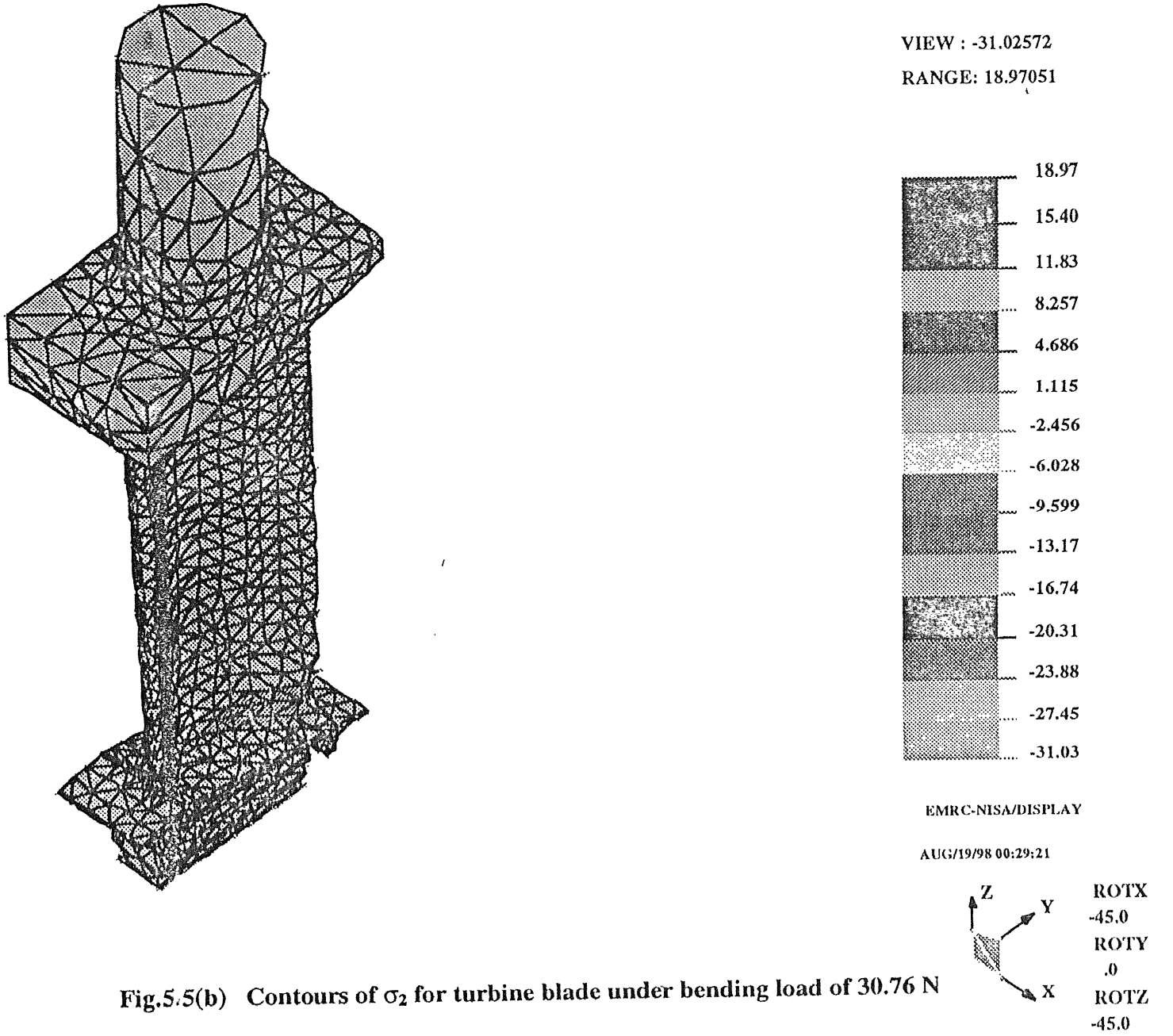

Fig.5.5(b) Contours of σ_2 for turbine blade under bending load of 30.76 N

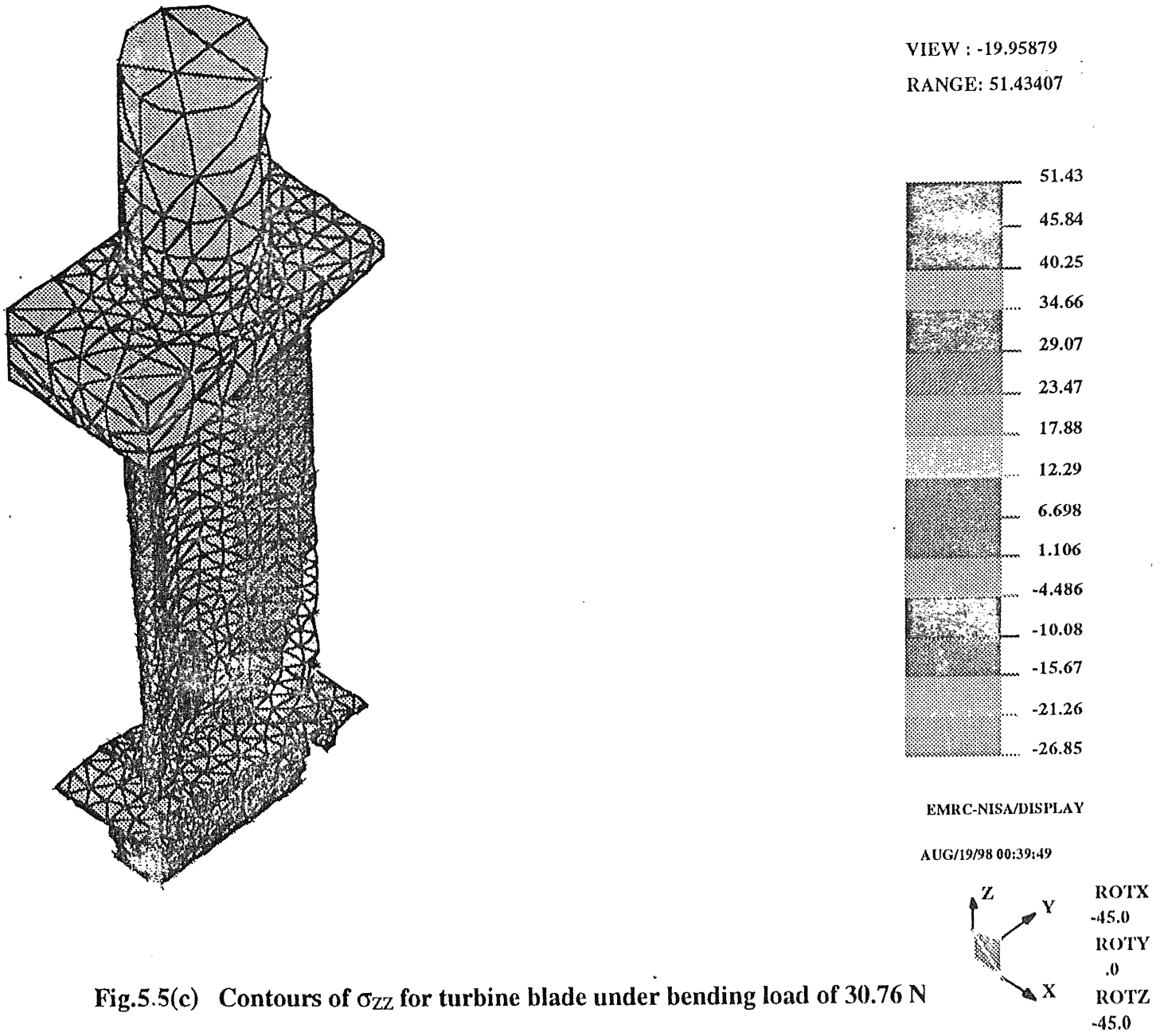

Fig.5.5(c) Contours of σ_{ZZ} for turbine blade under bending load of 30.76 N

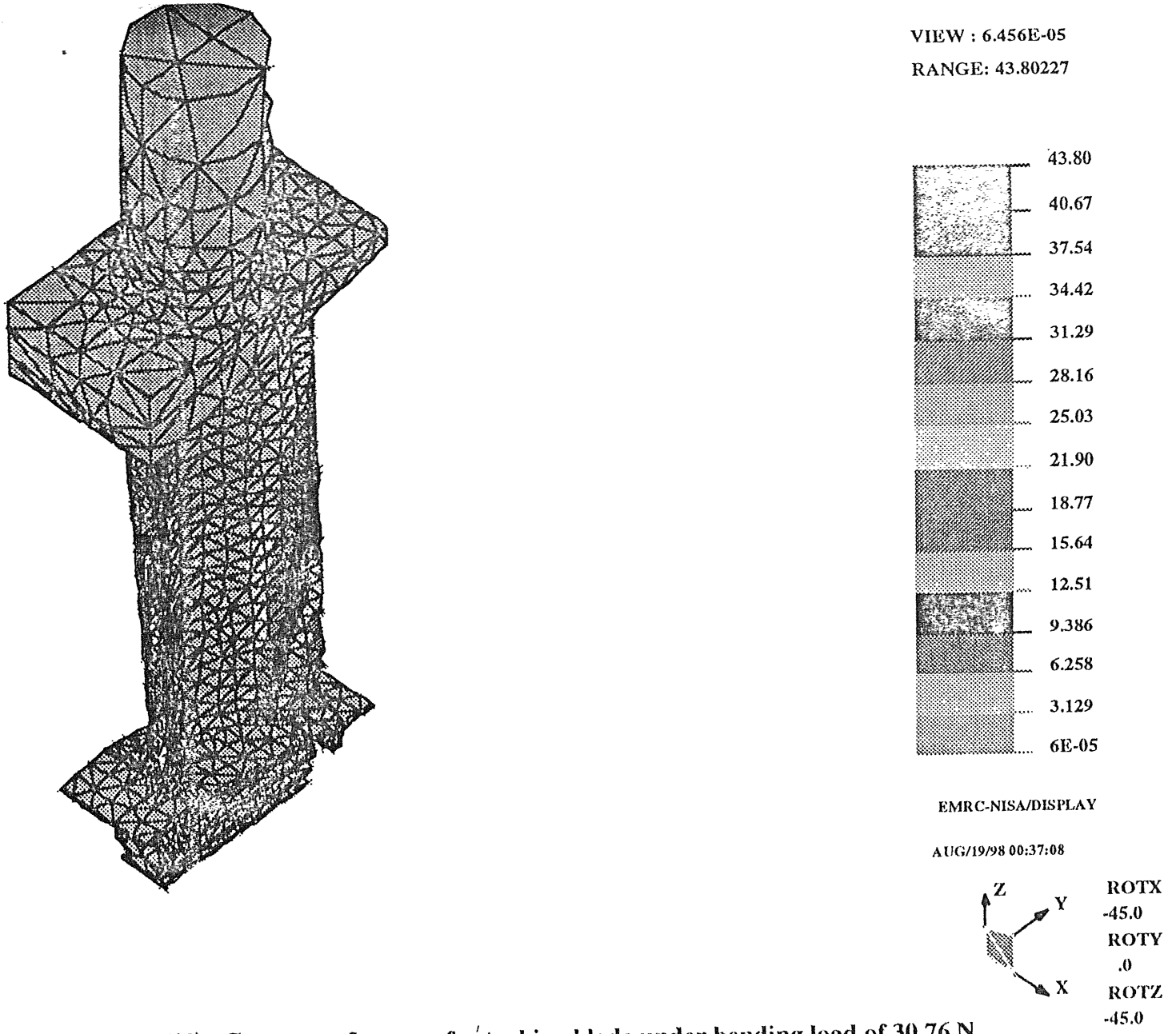

Fig. 5.5(d) Contours of σ_1 - σ_2 for turbine blade under bending load of 30.76 N

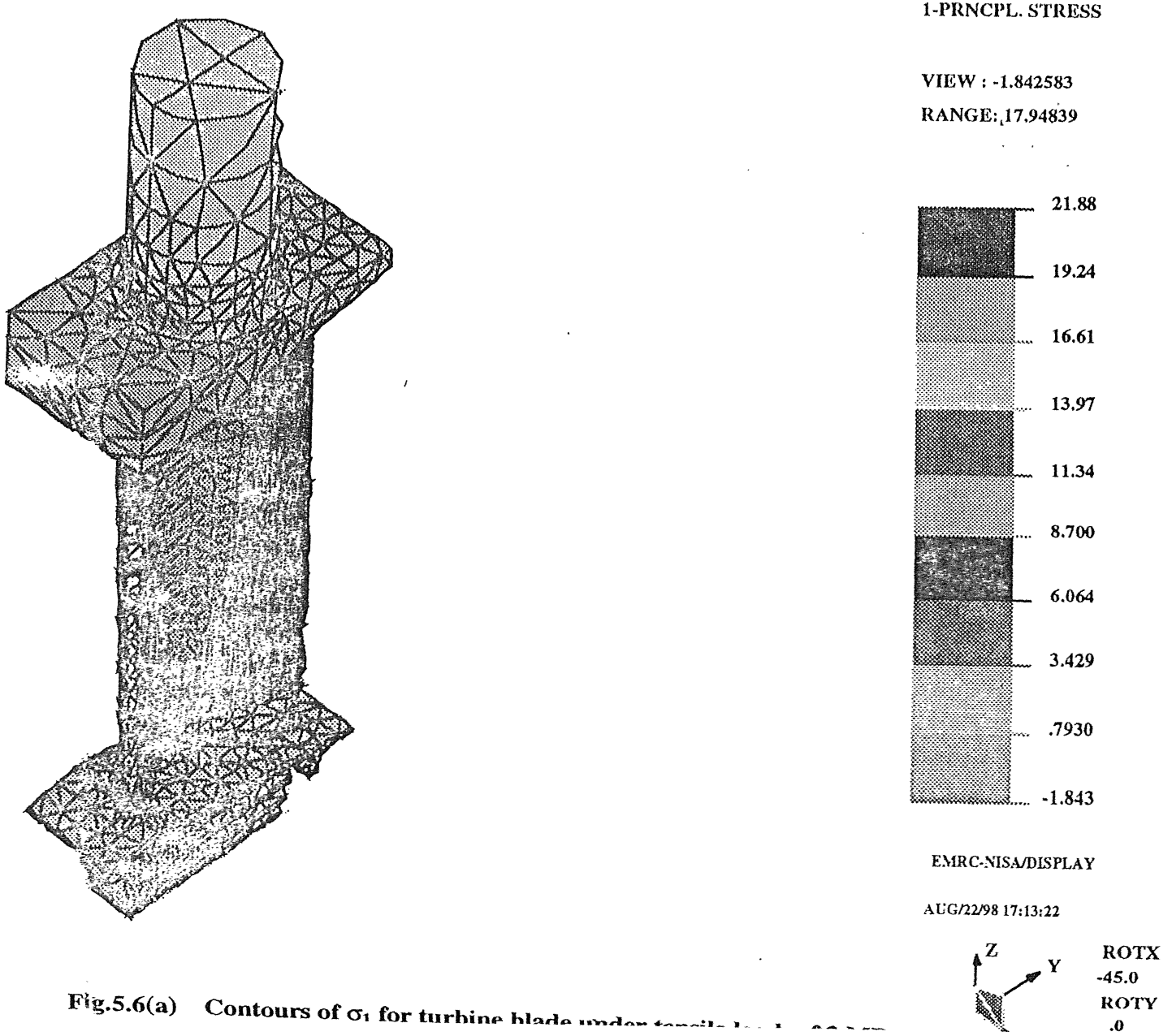

Fig.5.6(a) Contours of σ_1 for turbine blade under tensile l

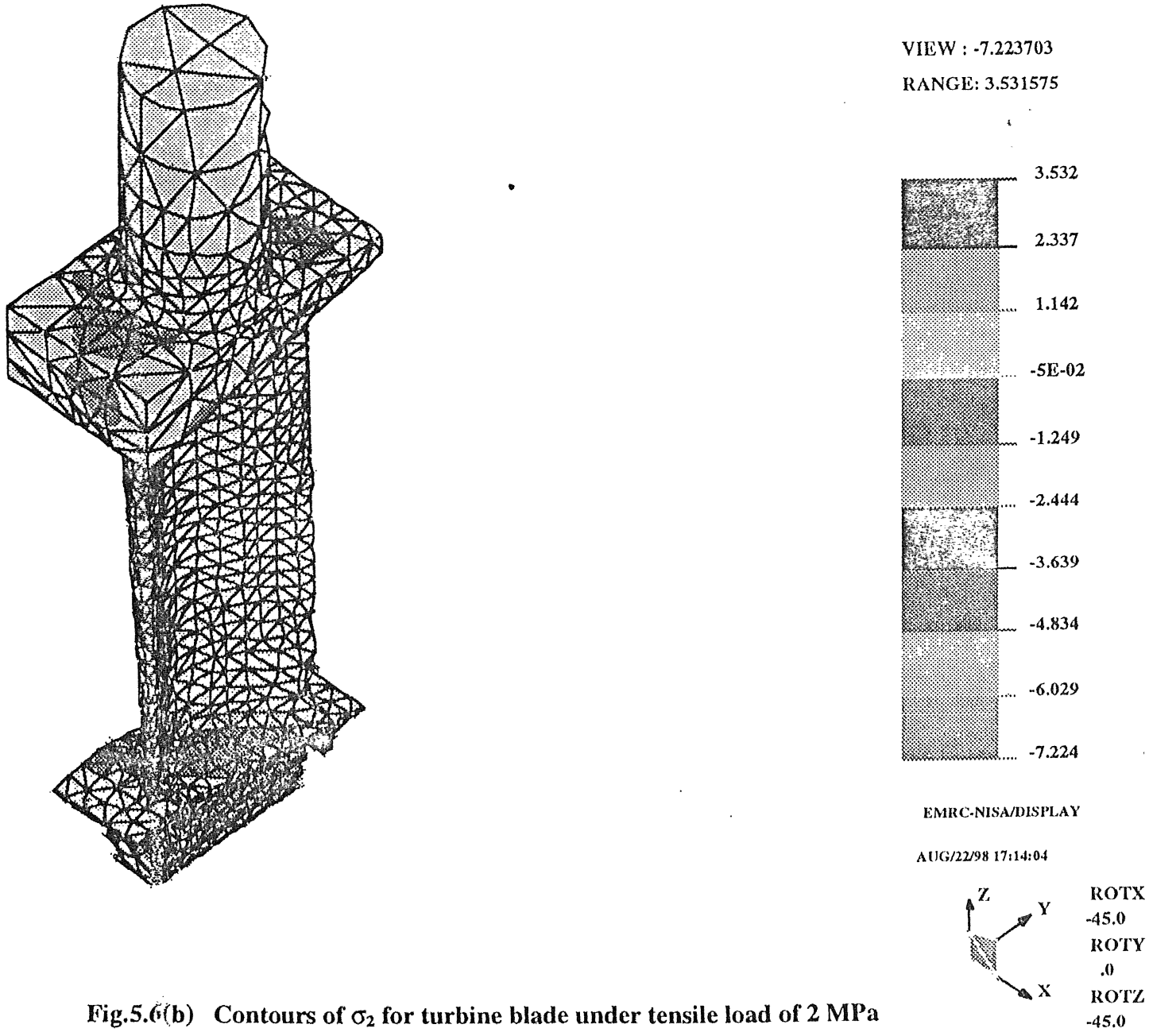

Fig.5.6(b) Contours of σ_2 for turbine blade under tensile load of 2 MPa

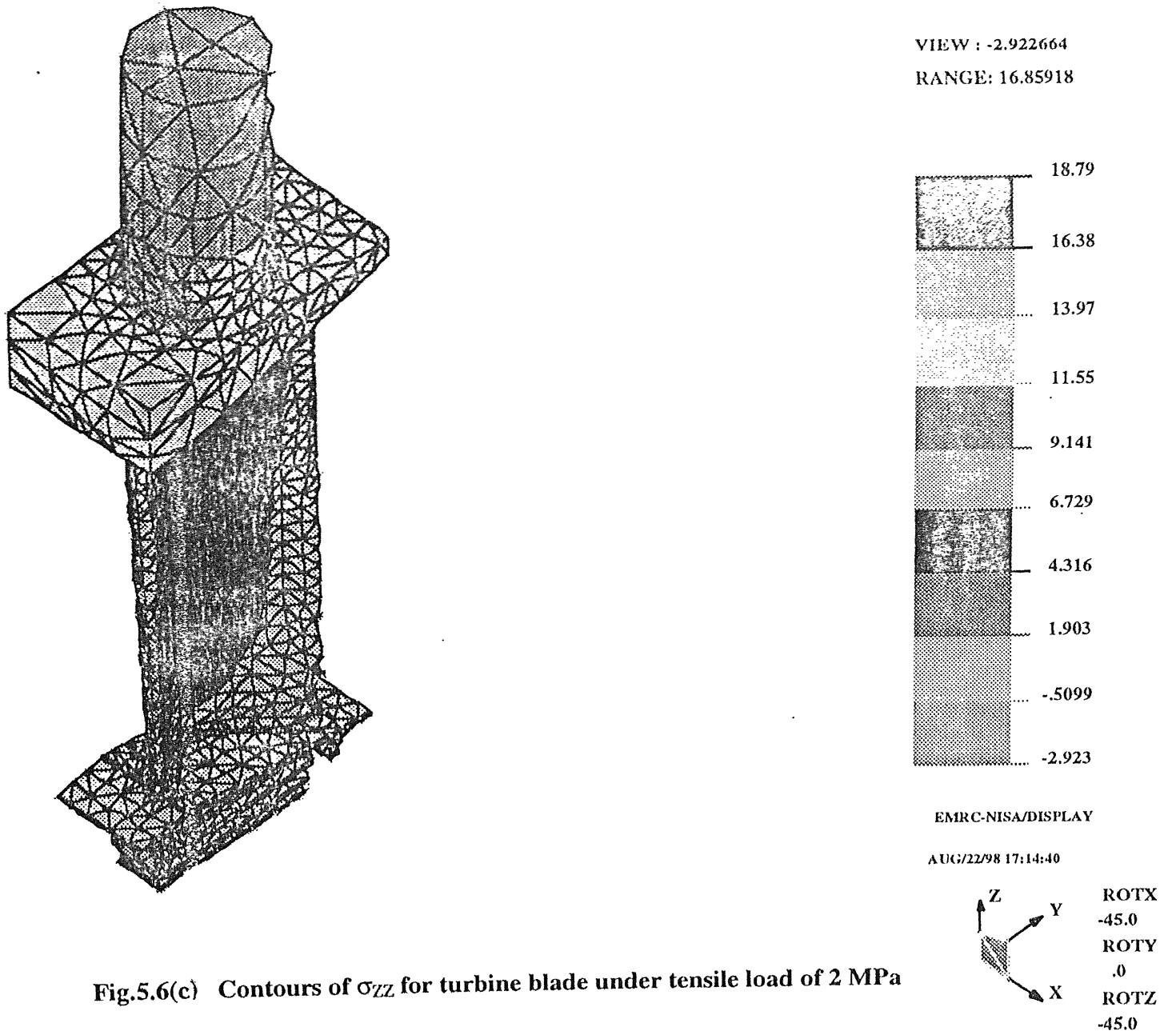

Fig.5.6(c) Contours of σ_{ZZ} for turbine blade under tensile load of 2 MPa

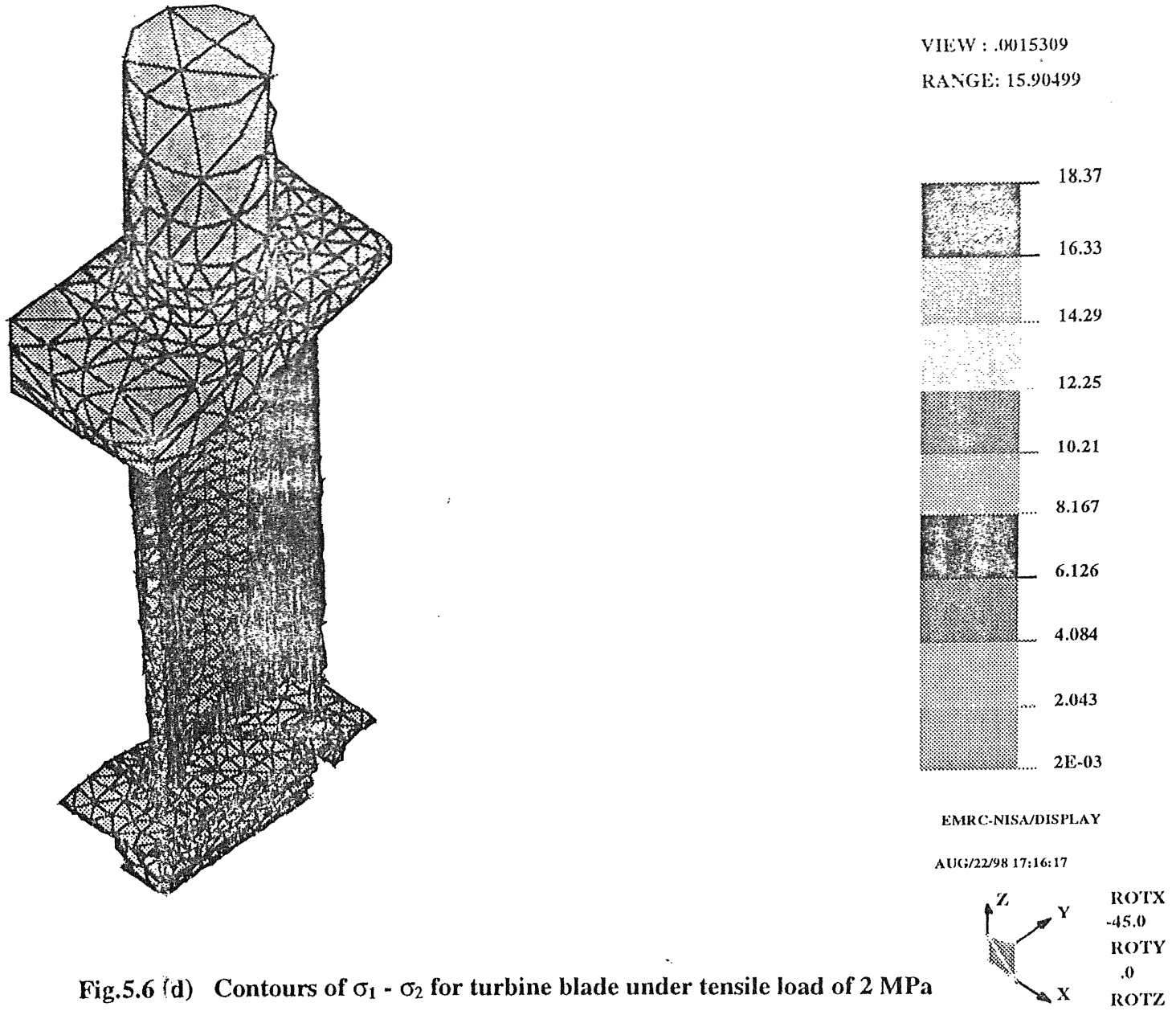

Fig.5.6 (d) Contours of σ_1 - σ_2 for turbine blade under tensile load of 2 MPa

Chapter 6

CONCLUSIONS

6.1 CASE STUDIES

In the present work an attempt has been made to look at the feasibilty to stress analysis of components made from the Rapid Tooling system. The objective was a whole field stress analysis of components at any stage of a product life cycle of a component. The input to photoelasticians is a 3D model of the component for analysis. Component making in a convetional methodology as a time cinsuming process and hence rapid Prototyping was chosen as a component making methodology.As the models made directly from the RT processes are not directly amanble to stress analysis RP based on FDM/SGC is coupled with the rapid tooling technology.

Two components were chosen for the present work, namely a circular disk and turbine blade. The whole work encompassing RP, Vacuum Casting and Photoelastic stres analysis posed a number of challenges which were overcome successfully.

6.2 TECHNICAL SUMMARY

RP technology has proved to be a boon for designers. Designers can have the model ready in virtually no time, which can be analysed using photoelastic techniques directly. The models made from the fused deposition modelling system are porous and this makes the silicone rubber used in vacuum casting process to enter the pores in the models made by FDM process. The removal of the component from the silicone mold becomes difficult when the siliocne gel enters the pores. In case of components with deep holes removal of components from the mold is more difficult. Sufficient care has to be taken in model preparation when using the FDM copmonent to ensure that the silicone rubber does not enter into the pores. As compared to the FDM process the SGC process gives solid components. They do not have the problem of porosity. Hence for components with deep holes SGC is to be preferred fo making the master pattern for the vaccum casting process. With new developments in the field of polishing and filling the FDM process these shortcomings can be easily overcome.

Molds have been succesfully made for a number of components of which the circular disk and tubine blade are used for the present analysis. The molds are made of silicone rubber. Sufficient care has to be taken in handling the siliocne rubber and the resins in preparing the mold and components. Flowability of silicone rubber decreases with time once it is mixed with the catalyst. Uniform mixing of the silicone rubber and catalyst is to be ensured without which the cross-linking of chains in the material would not be uniform and the silicone rubber will not solidify uniformly throughout the volume. The whole process of pouring the mold is to be completed in 70 minutes from the point of adding the catalyst. The primary degasiing time for the silicone is to be kept as low as possible as the flowability decreases with time. Due to this the silicone gel will not be able to enter deep pathches.

The reaction between SG95A and SG95B is an exothermic effervescent reaction. If the curing temp is reduced it has been observed that a lot of bubbles form in the end component.

Enough care has to be given to the gate/sprue design. If the gates/sprues are made too small the flow of resin into the mold causes early setting of the resin before mold is full. Bubbles will also get trapped in the resin.

Photoelastic analysis has been successfully applied to the models cast from the silicone molds. The material was standardized using a circular disk under diametral compression. The F_σ value was found to be 7.5 N/mm per fringe. The circular disk was also analyzed for doing 3D photoelastic stress analysis using stress freezing technique. This particular resin was also amenable to stress freezing as explained in this work. A major hindrance to the analysis was the high amount of residual stresses that are being locked in the model. This was improved upon after a lot of experimentation by changing the ratio in which the two components of the resin SG95 are mixed. The actual ratio was 2:3 of resin SG95 A and SG95 B and this ratio was changed to 1.6:3 and 1.75 : 3 to look at the variation of residual stresses. There was a lot of improvement in the model. The stress freezing of these circular disks with different ratios was also undertaken. The stress freezing of the circular disk made with 1.6:3 of SG95 A and SG95 B did not yield good results. The fringe bands were very thick and

non-uniform. This problem has to be investigated by using higher loads. Different other ratios are to be tried out.

6.3 SUGGESTIONS FOR FUTURE WORK

=> Better techniques are to be developed to improve the surface finish of the model. The greater the surface finish of the model the higher is the transparency of the model.

=> The stress freezing ability of the SG95 resin has been established. More complex models need to be analyzed by following the slicing procedure and using stress separation techniques real time problems need to be solved.

=> Although the residual stresses have been considerably reduced various other ratios are to be tried out to still reduce the residual stress.

=> There are other silicone vacuum casting systems where in the silicone is cured by Ultraviolet light. These are one component systems. Even the resins used in this process are one component systems. Being one component systems these resins might not develop the residual stresses because of the cross-linking between the atoms. This can be tried out although it is a costly process.

=> Polariscope elements (polarizer, analyzer, quarter wave plates) need to be of higher quality to enable one to measure the fringe orders near stress concentration zone.

=> Elastic properties of the SG95 models should be evaluated accurately with experimental techniques under actual service conditions prior to the stress analysis.

=> In case of FEM analysis one should find a way to implement more stringent boundary conditions for a particular problem with correct FEM modelling.

[1] Steven Ashley, "Prototyping with advanced tools", *Mechanical Engineering*, June 1994, pp 48-55.

[2] Pham and Gault R.S., "Modelling for all occasions", *Manufacturing Engineer*, December 1996, pp 289-293.

[3] Dhande S. G., "Rapid Tooling Lecture Notes", *CAD Project, I.I.T. Kanpur*, 1998.

[4] Dally J.W. and Riley W.F., "Experimental stress analysis", *McGraw Hill Inc.*, 1991.

[5] FDM System Documentation by Stratasys Inc., May 1996.

[6] Solider System Documentation by CUBITAL Inc., Israel, Jan 1998.

[7] Karatis, N. P., van Grithuysen, J.-P.S., and Glardon, R ., "Direct Rapid Tooling: a review of current research", *Rapid Prototyping Journal*, Vol.2, No. 4, June 1998, pp 77 - 89.

[8] MCP Vacuum Casting System Documentation by HEK GmbH, Germany., Jan 1998.

[9] Ramesh K. and Muralidhar K., "Computer applications in experimental mechanics", 1994.

[10] Ramesh, K., ganesan, V.R. and Mullick, S.K., "Digital image processing of photoelastic fringes - a new approach", Experimental Techniques, Vol.15, No. 5, 1991, pp 41-46.

[11] Ramesh, K., and Mangal, S.K., "Data Acquisition Techniques in Digital Photoelasticity : A review", *Opt. And Lasers In Engg.*, (in press)

[1] Kai C.C. and Fai L.K., "Rapid Prototyping - Principles and Applications", *Wiley Eastern New York*, 1996.

[2] Fadel G.M. and Kirchman C., "Accuracy issues in CAD to RP translations", *Rapid Prototyping Journal*, Vol.2, No.2, 1996, pp 4-17.

[3] Dhande S. G., "CAD and Prototyping Lecture Notes", *CAD Project, I.I.T. Kanpur*, 1997.

[4] Masood, Syed H., "Intelligent Rapid Prototyping with Fused Deposition Modelling", *Rapid Prototyping Journal*, Vol.2, No.1, 1996, pp 24-33.

[5] Ghosh A., "Rapid Prototyping", *EWP*, 1996.

[6] Dolenc A. And Makela I., "Slicing procedure for layered manufacturing techniques", *Computer Aided Design Journal*, Vol.26, No.2, Feb 1994, pp 119-126.

[7] Jessop H.T., "On the Tardy and Senarment methods of measuring fractional relative retardations", *British Journal of Applied Physics*, Vol.4, 1953, pp 138-141.

[8] Fordham S., "Silicones", *George Newness Limited*, 1960.

[9] Handbook on Experimental Mechanics, *Society for Experimental Mechanics*, 1987

[10] Reddy J.N., "An introduction to finite element analysis", *McGraw Hill*, 1993.

[11] Pathak P.M., "Photoelasticity and Finite Elements - Complimentary Tools in Stress Analysis", *Thesis submitted to Dept. of Mechanical Engg., I.I.T. Kanpur*, January 1998.

[12] Ramesh K., Yadav A.K. and Pankhawalla V.A., "Plotting of Fringe Contours from Finite Element Results", *Communications in numerical methods in engineering*, Vol.11, 1995, pp.839-847.

[13] NISA Manuals by EMRC.

APPENDIX 1

Fig 4.8 explains the variation in the residual stresses of the component made from the silicone molds with different ratios of the SG95 resin. SG95 resin comes as a two component resin of SG95 A and SG95 B. The ratio in which these two are mixed is 2:3, as prescribed by HEK GmbH, GERMANY. In this work the ratio in which these two are mixed, is varied from 2:3 to 1.75:3 and 1.6:3, to study the change in residual stress. The results of this analysis are clearly shown in the Fig 4.8. In figure 4.8 (a) (i) and (ii) the dark and bright field images of the residual stresses in the turbine blade for a ratio of 2:3 are shown. The Fig. 4.8 (a) (iii) and (iv) shows the fringe pattern of the turbine blade when a load of 30.76 N is applied. No preliminary analysis was carried out after applying the load on the model as the model was very thin at the root due to which it cannot carry higher loads. According to the color code in digital photoelastic techniques the amount of the residual stress in the turbine blade is of the order of 3. This is reckoned to be a very high amount of residual stress in the turbine blade and the analysis of the component with such a high amount of residual stress would lead to erroneous results.

The next set of experiments were carried out by changing the ratio in which the two components are mixed to 1.75:3. The results are shown in the Fig. 4.8 (b). The Fig. 4.8(b) (i) and (ii) are the dark and bright field images of the turbine blade under no load conditions. As compared to the blade with a ratio of 2:3 the amount of residual stress in the this case is less. The fringe order is less than that in Fig. 4.8 (a). The Fig. 4.8 (b) (iii) and (iv) demonstrates the response of the resin when a load of 30.76 N is applied.

With encouraging results coming out of the change in ratio of SG95 A and SG95 B to 1.75:3, the ratio has been decreased further to understand the effect of the change in the ratio. The ratio was changed to 1.6:3 in the last attempt. Fig. 4.8 (c) (i) and (ii) demonstrate the response of the resin. The residual stresses in the component

have come down significantly. The amount of residual stress present in this case is negligible and these components can be readily used for analysis. The behavior under load of the turbine model is shown in Fig 4.8 (c) (iii) and (iv).
